doi:10.20944/preprints201907.0018.v1

Article

Identification of Hub genes and key pathways associated with atopic dermatitis via Integrated Bioinformatics

Yue Sun, Angela Weihong Yang and George Binh Lenon*

[1] School of Health and Biomedical Sciences, RMIT University, Victoria, Australia
*Correspondence: George.lenon@rmit.edu.au

Abstract: The exploration and identification of targets and pathways for Atopic dermatitis (AD) treatment and diagnosis are critical for AD control. The conventional target exploration approach such as the literature review is not satisfying in terms of efficiency and accuracy. Recently, the bioinformatic approach is drawing attention for its unique advantage of high-volume data analysis for target and pathway exploration; Open Targets Platform is the targets source for this study to extract top 200 high-rank proteins from 3122 AD associated proteins. STRING, Cytoscape, CytoHubba, ClueGo, and CluePedia function had been applied for data analysis. The KEGG Mapper search & colour pathway was the pathway map resource for identified pathways; 23 key hub genes (VDR, KIT, BCL2L11, NFKBIA, KRAS, IL13, JAK2, STAT3, IL21, IL4R, REL, PDGFRB, FOXP3, RARA, RELB, EGFR, IL21R, MYC, CREBBP, NR3C1, IL2, JAK1, and KITLG). Additionally, 8 correlated pathways and the biological process had been identified; Through this study, a viable approach for target and pathway exploration had been presented. The identified AD targets and pathways will be tested for upcoming research for traditional Chinese medicinal herb interactions.

Keywords: Atopic Dermatitis; AD; Dermatology; target identification; pathway identification; Bioinformatics; Protein-protein networks.

---

1. Introduction

Atopic dermatitis (AD) is a long-lasting and relapsing skin inflammation disease characterized by itchiness, dry skin, and red crusted skin lesions [1]. In the developed countries, the prevalence rate of AD is about 10-25% and 2-8% in children and adults, respectively [2]. AD is often associated with other atopic conditions including allergic rhinitis, asthma, and food allergies [3]. The repercussions of this disease are tremendous and detrimental in terms of quality of life and social-economic impacts. The multi-faceted pathogeneses of AD which included itchiness, skin barrier dysfunction, innate immune response, adaptive immune response, and inflammations [4]. AD has a significant difference between acute stage and chronic stage in terms of age groups and severity levels [5]. Therefore, it is crucial if these four pathogenic roles can be elucidated with stage differentiation. Despite the exploration of these existing information, the treatment outcome is still unsatisfactory when it comes to moderate-to-severe cases. The immunosuppressant could restrict the severity level of AD at the price of off-target effects, safety and tolerability concerns [6]. Therefore, the desire for target exploration and pathway analysis is still advocated to optimize AD management. The identification of hub genes, enrichment of the key pathways, and visualization of the network of hub genes will provide more accurate and reliable therapeutic and diagnostic targets for AD control.

2. Experimental Section

2.1 Target protein identification and selection

The AD-associated target proteins had been extracted from the online database "Open Targets Platform" (https://www.opentargets.org/). By far, it is one of the most sophisticated online databases which presents the human genetic data and associated diseases supported by a unique rating system which incorporate several parameters from the genetic association, somatic mutations, drugs, pathways & systems biology, RNA expression, text mining, and animal models. The overall scores are available for quantitative selection. The target confidence level is supported by these 7 evidence systems. Therefore, the high overall score is preferred in this study. The below keywords had been utilized for AD target protein search in the database: "Atopic dermatitis" and "Atopic Eczema".

2.2 Target proteins analysis

The selected target proteins had been processed by STRING (https://string-db.org/) to demonstrate their protein-protein interactions. The nodes with connections were selected for further analysis.

2.3 Hub genes identification and their Pathway enrichment

*Cytoscape 3.7.1 version software was applied to visualize the protein interaction relationship network and analyse hub proteins which are important nodes with many interaction partners. To pinpoint the hub genes, an application named CytoHubba in this software had been employed with five algorisms: Degree, Edge Percolated Component or EPC, Maximal Clique Centrality (MCC), Maximum Neighbourhood Component (MNC), and one of the Centrality functions EcCentricity. The target protein can be viewed as the hub gene if the degree value >10 [7]. The top 50 proteins in each algorism had been analysed by Venn diagram via "Bioinformatics & Evolutionary Genomics" (**http://bioinformatics.psb.ugent.be/webtools/Venn/**). The hub genes had been further analysed by other applications from Cytoscape named ClueGo and CluePedia to illustrate the key pathways and their proportions. The pathway settings were chosen from GO Biological Process, GO Cellular component, GO Molecular function, KEGG, and REACTOME-Pathways. The selected pathways must satisfy P-value ≤ 0.05. The identified key hub gene names were transferred into UniProt (https://www.uniprot.org/) entry names for KEGG Mapper search & colour pathway (**https://www.genome.jp/kegg/tool/map**) to identify the key pathway maps with involved targets highlighted with yellow colour.*

3. Results

3.1 Target proteins identification and selection

From Open Targets platform search, the below result terms have been presented as "Atopic Eczema". Totally, 3122 targets had been identified from Open Targets platform. The top 200 targets were selected by the overall score. The top 200 targets from Open Targets Platform have been summarized in the supplement table 1.

3.2 Target proteins analysis

In STRING analysis, 200 input target proteins generated 197 matched results with three unidentifiable proteins named immunoglobulin heavy constant mu (IGHM), AC116366.3, and testis expressed basic protein 1 (TSBP1). The selection cut-off value was set at 0.400 which is medium confidence score. The graph in Figure 1 Shows the dense connections among these 173 target proteins and 24 targets without connection in the network. The 173 targets formed a network by Cytoscape with table panel provided a series of parameters results including Average shortest path length, clustering coefficient, closeness centrality, Eccentricity, Stress, Degree, Betweenness centrality, neighborhood connectivity, radiality, and topological coefficient. Among these parameters, Degree is the most significant parameter. It indicated 63 targets with results higher than 10 marks, 110 targets were less than 10 marks. The table panel results had been extracted into supplement table 2. The degree differentiation had been transformed into a network with color variety in Figure 2.

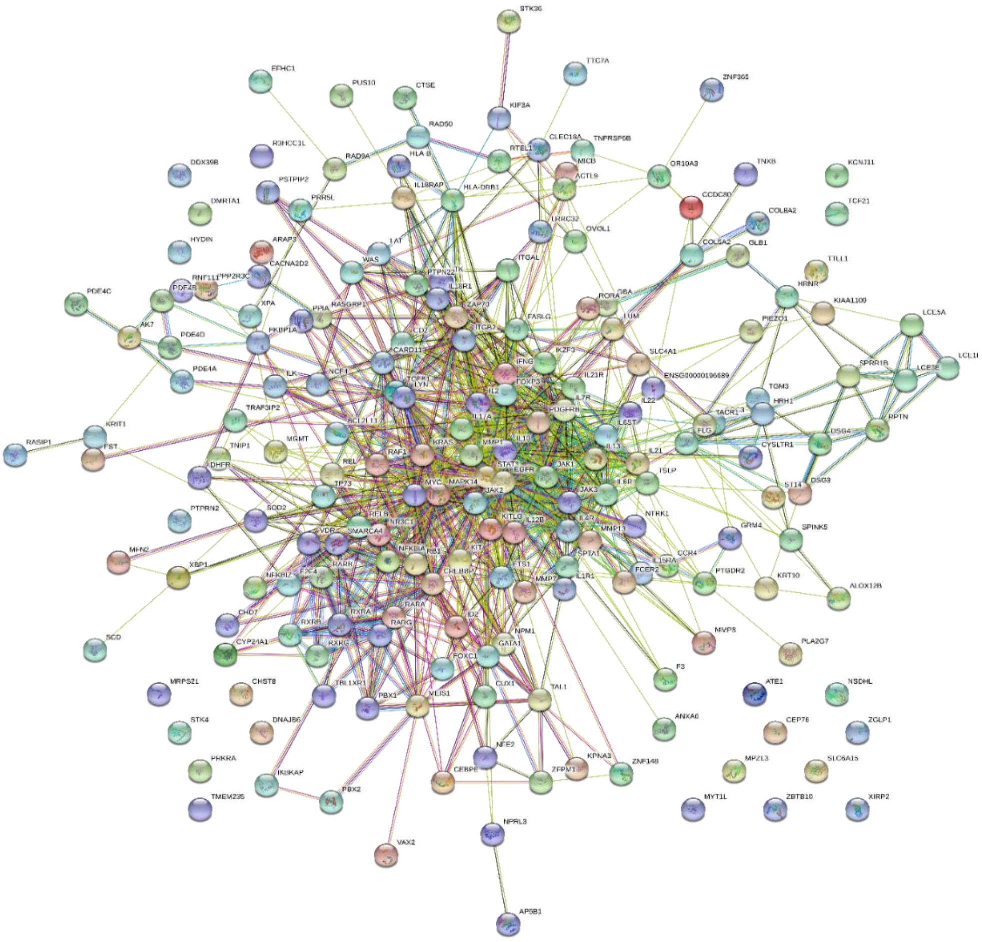

Figure 1. STRING network of 197 target proteins. Number of nodes: 173, number of edges: 981. PPI enrichment p-value:< 1.0e-

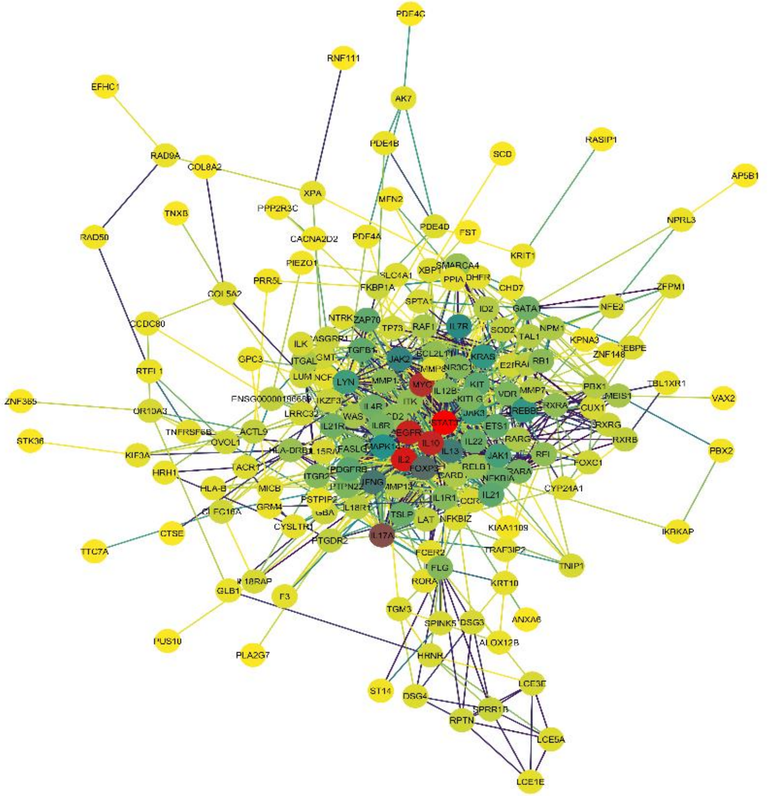

Figure 2. Cytoscape network for 173 nodes (target proteins) with colour differentiation by different Degree value. The high degree targets are concentrated in the middle of the graph. The red coloured nodes are the top five high degree proteins.

3.3 Hub genes identification and their Pathway enrichment

*The top 50 target proteins in each mentioned algorism had been integrated for key hub genes. The 23 hub genes had been presented in **Figure 3**. The results from each algorism had been presented in **supplement table 3**. The pathways associated with 23 hub genes had been analysed by ClueGo and CluePedia. The results had been generated to visualize the pathway connections among the hub genes in **Figure 4 (a)**. The proportions of pathways and key pathways had been showcased in **Figure 4 (b)** and **Figure 4 (c)**, respectively. The pathway maps extracted via KEGG Mapper are associated with the JAK-STAT signaling pathway, Th17 cell differentiation, and the Notch signaling pathway in **Figure 5**.*

VDR (degree value: 19), KIT (24), BCL2L11 (16), NFKBIA (22), KRAS (30), IL13 (37), JAK2 (35), STAT3 (62), IL21 (24), IL4R (21), REL (16), PDGFRB (24), FOXP3 (40), RARA (20), RELB (15), EGFR (55), IL21R (21), MYC (52), CREBBP (30), NR3C1 (18), IL2 (57), JAK1 (27), and KITLG (19) are the identified key hub genes. In the network of key pathways, there are 173 Nodes and 981 Edges.

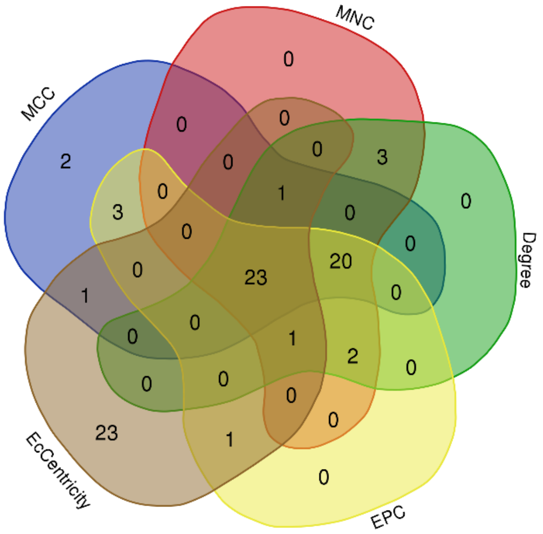

Figure 3. the Venn diagram for 23 key hub genes integrated by the results of algorism of MCC, EcCentricity, EPC, MNC, and Degree. The elements in concurrent areas are the 23 hub genes (VDR, KIT, BCL2L11, NFKBIA, KRAS, IL13, JAK2, STAT3, IL21, IL4R, REL, PDGFRB, FOXP3, RARA, RELB, EGFR, IL21R, MYC, CREBBP, NR3C1, IL2, JAK1, and KITLG)

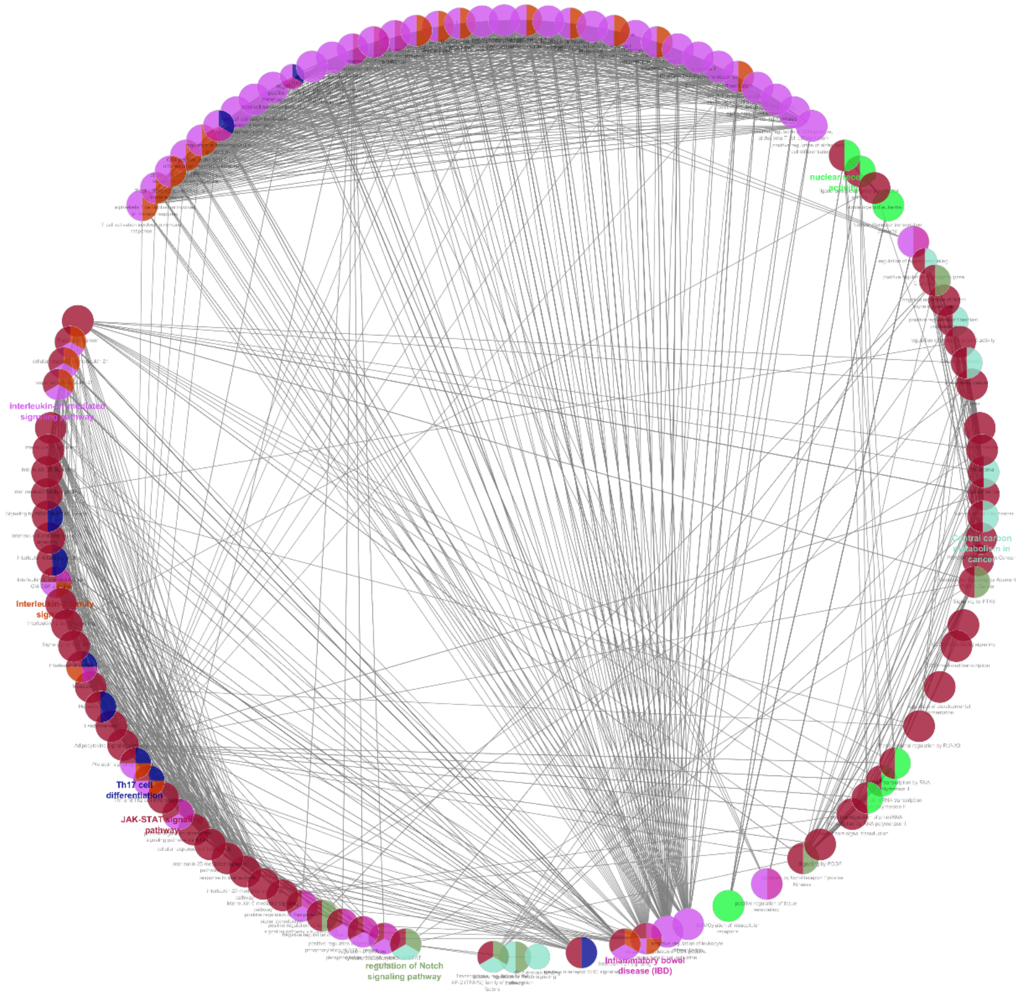
nuclear receptor activity
interleukin-21-mediated signaling pathway
cellular response to interleukin-21
Interleukin-2 family signaling
Central carbon metabolism in cancer
Melanoma
Bladder cancer
Signaling by PTK6
Th17 cell differentiation
JAK-STAT signaling pathway
regulation of Notch signaling pathway
Inflammatory bowel disease (IBD)

(a)

doi:10.20944/preprints201907.0018.v1

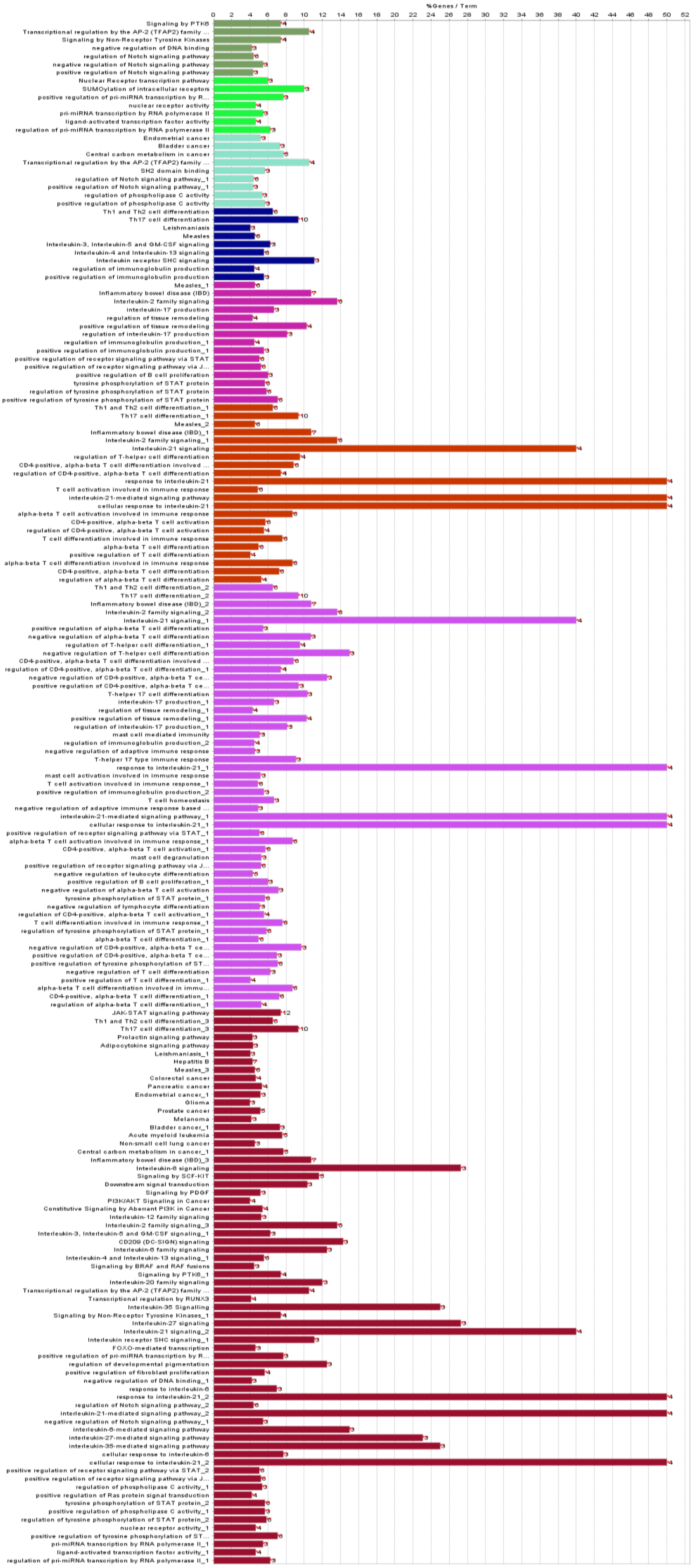

(b)

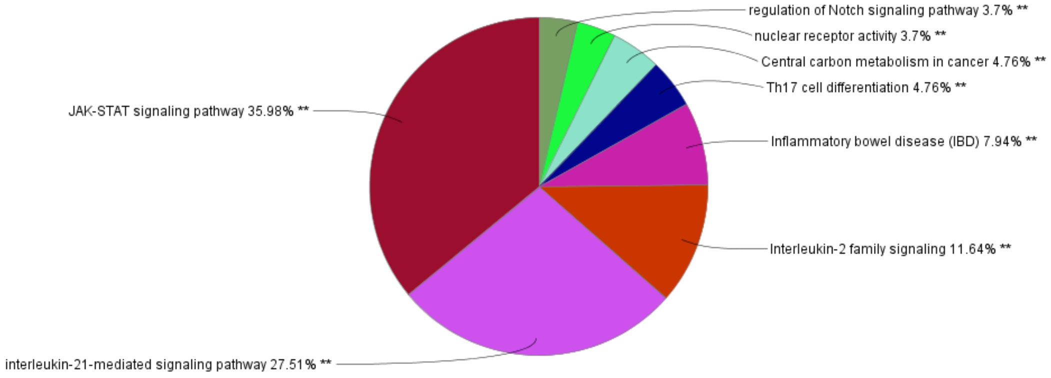

(c)

Figure 4. ClueGO and CluePedia analysis: (a) the network of key pathways associated with 23 hub genes. The eight key pathways had been highlighted with different colour. (1). JAK-STAT signalling pathway in dark red. 2. Interleukin-21-mediated signalling pathway in light pink. 3. Interleukin-2 family signalling in light red. 4. Inflammatory bowel disease (IBD) in dark pink. 5. Th17 cell differentiation in blue. 6. Central carbon metabolism in cancer. 7. Nuclear receptor activity. 8. Regulation of Notch signalling pathway (b) the bar chart of pathways for 23 key hub genes associated with AD, P-value≤0.05. (c) the pie chart of 8 major pathways (1. JAK-STAT signalling pathway 35.98%. 2. Interleukin-21-mediated signalling pathway 27.51%. 3. Interleukin-2 family signalling 11.64%. 4. Inflammatory bowel disease (IBD) 7.94%. 5. Th17 cell differentiation 4.76%. 6. Central carbon metabolism in cancer 4.76%. 7. Nuclear receptor activity 3.7%. 8. Regulation of Notch signalling pathway 3.7%.

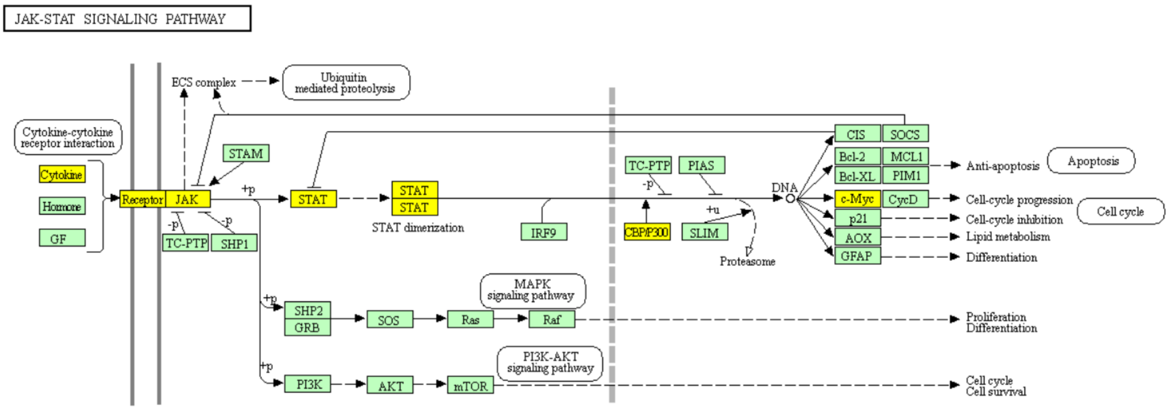

(a) Cytokine includes IL-2, IL13, and IL21; Receptor includes IL4R and IL21R; STAT includes STAT3; CBP/P300 includes CREBBP; c-Myc: MYC

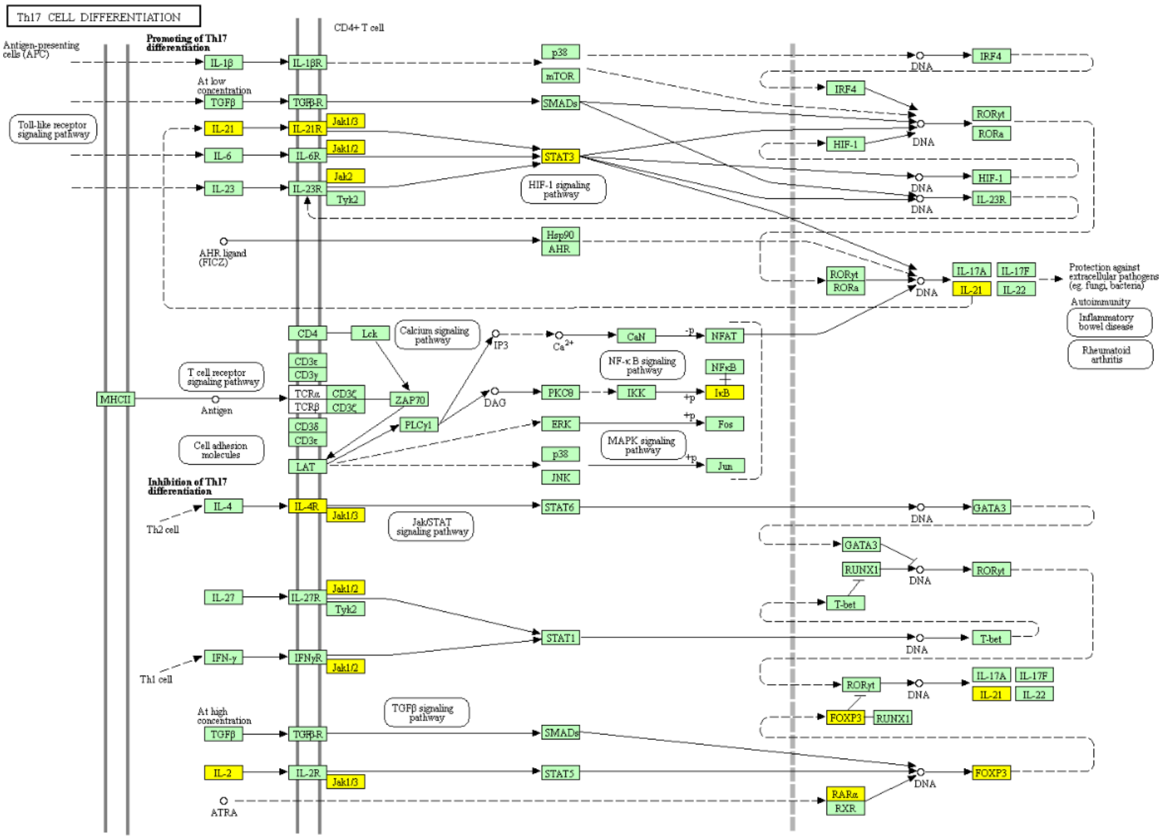

(b) IκB includes NFKBIA

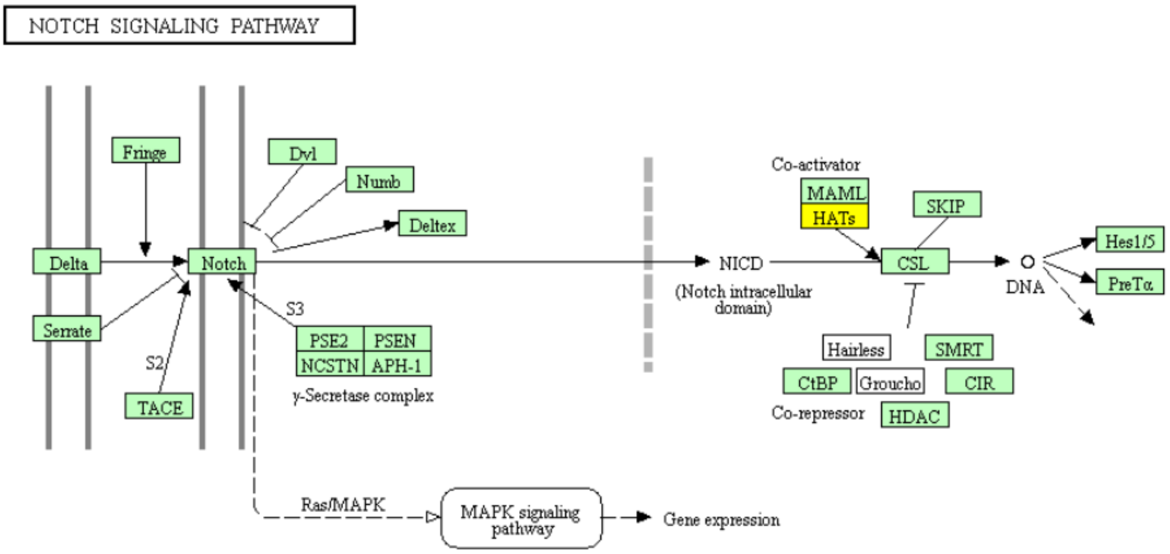

(c) HATs Includes CREBBP

Figure 5. (a) JAK-STAT signalling pathway, (b) Th17 cell differentiation (c) Notch signalling pathway extracted from KEGG Mapper. The key hub genes were highlighted in yellow colour.

4. Discussion

Identified pathways

The three pathways identified by KEGG Mapper play irreplaceable roles in the pathogenesis of AD.

For the JAK-STAT signal pathway, it participates in Th2 immune driven cytokines downregulation for IL-4, IL-5, and IL-13. Additionally, it involves the exaggeration of Th2 cell response, activation of eosinophils, maturation of B cells, suppression of regulatory T cells, epidermal chemokines pro-inflammatory cytokines, and pro-angiogenic factors upregulation, antimicrobial peptides downregulation, and skin barrier function [8]. In the clinical phase, the testing medication tofacitinib had yield impressive result from patients with moderate-to-severe AD. Specifically, tofacitinib 5mg daily or twice daily could achieve a 66.6% reduction in severity scoring of AD (SCORAD) and a 69.9% remission in pruritus and insomnia scores. Another trial performed even better by conducting on a larger sample group of AD patients with 81.7% reduction in Eczema Area and Severity Index (EASI) in comparison with the control group with only 29.9% reduction. Besides, there are more trials are underway to prove the efficacy of new medications such as Baricitinib and Ruxolitinib by targeting this pathway. IL-2, IL13, and IL21 are the Cytokines involved in the cytokine-cytokine receptor interaction. IL-2 produced by T-cells in response to antigenic or mitogenic stimulation, this protein is required for T-cell proliferation and other activities crucial for the regulation of the immune response. It can stimulate B-cells, monocytes, lymphokine-activated killer cells, natural killer cells, and glioma cells. New medicine Apremilast in the clinical trials for AD management is tailored for IL-2. IL-13 inhibits inflammatory cytokine production and synergizes with IL2 in regulating interferon-gamma synthesis. Therefore, it may be critical in regulating inflammatory and immune responses. Tralokinumab and Lebrikizumab are medication by targeting IL13.

For Interleukin-21-mediated signaling pathway, IL21 and IL21R are found to have high expression in skin lesions of AD patients. It had been found the productions of IL21 mostly came from mononuclear leukocytes penetrating the epidermis and less from cells penetrating the epidermis [9].

As for inflammatory bowel disease (IBD), In professor Jochen's retrospective cohort study conducted on 655815 patients, the patients with AD have significantly increased comorbidities of developing IBD and rheumatoid arthritis (RA) in comparison with the controls without AD. It is echoed that genetic predetermination in AD could be the reason for immune abnormalities which occur on AD, IBD, and RA. Therefore, AD is a risk factor for the development of IBD and RA [10].

For Th17 cell differentiation, it involved multiple identified targets including IL21, IL21R, JAK1, JAK2, STAT3, IL4R, NFKBIA, IL2, FOXP3, and RARA. This biological process contributed to the treatment of AD and a series of other autoimmune diseases [11].

As for Nuclear receptors, they are a family of proteins which could interact with ligands involving in the steroid, thyroid hormones, retinoids, and certain molecules production. Their functions are to regulate the expression of specific genes [12]. The clinical trial results support the claim of bexarotene gel which aims nuclear receptors as medication target for inflamed severe hand dermatitis management [13]. Thus, nuclear receptor activity may be one of the possible biological processes for AD pathology.

The deficient epidermal Notch signaling pathway in AD leads to viral infection, Staph.aureus colonization, inflamed skin pruritus, type-1 hypersensitivity, inflammation, and atopic dry skin [14]. CREB binding protein (CREBBP) or (CBP) participates in this pathway. For AD pathogenesis study, an animal experiment proved involucrin's expression and IL-4 target gene expression can be modulated by CREBBP in AD skin barrier defects [15].

The most enriched pathway map extracted by professor Zhang et al about AD key genes screening was the Chemokine signalling pathway which presents by chemokine (C-C motif) receptor (CCR7), chemokine (C-C motif) ligand 19 (CCL19), signal transducer and activator of transcription 1 (STAT1) and phosphoinositide-3-kinase regulatory subunit 1 (PIK3R1) [16]. Our key hub genes are also involved in this pathway by the representation of the different set of genes which include Janus kinase 2 (JAK2), signal transducer and activator of transcription 3 (STAT3), GTPase KRas (KRAS), and NF-kappa-B inhibitor alpha (NFKBIA).

Identified targets

In rat AD model, Vitamin D receptor (VDR) deficiency had caused increasing trans epidermal water loss on epidermal barrier disruption with other known skin barrier related proteins reduction which include filaggrin, loricrin, and involucrin. Additionally, VDR enables to downregulate the expression of proinflammatory cytokines including interleukin-6, and tumour necrosis factor-α immune cells and impede maturation of dendritic cells. Therefore, by implementing the above-mentioned roles, VDR can exacerbate cutaneous bacterial infection in severe cases of AD [17]. Cholecalciferol or Vitamin D3 could be the representative medication aiming this target for AD treatment.

Tyrosine kinase transmembrane receptor (KIT) and Kit ligand (KITLG) which affiliates to stem cell factor (SCF) play an important role in the recruitment and proliferation of mast cells. As a receptor to SCF which also participates mast cell growth, migration, and differentiation. In the clinical trial, it has been found that SCF and KIT levels were strongly associated with AD severity and dropped after topical corticosteroids application. It is reasonable to apply KIT and SCF as biomarkers for AD severity assessment [18].

Bcl-2-like protein 11 (BCL2L11) is also known as Bim. Its expression and activity were modulated at the transcriptional and post-translational levels, coordinated expression and activity of immune responses and tissue integrity [19]. Its correlation with AD had been vindicated by a 3328 subjects' study with 14992 controls in Japan [20].

NFKB Inhibitor Alpha (NFKBIA) belongs to the family of NFKB inhibitors which proven to be an important molecular target for AD management through inflammatory related cells culture in vitro and allergic inflammation in NC/NgaTnd mouse in vivo [21].

From the description of the Open Targets platform, KRAS proto-oncogene, GTPase (KRAS) has the genetic association with AD. The mRNA expression of KRAS was observed in diabetic wound healing model with extracorporeal shockwave therapy in comparison with diabetic control. The result also confirmed the correlation with vascular endothelial growth factor (VEGF) which could be regarded as a potentially important mediator in the pathogenesis of AD [22,23]. Since the similarity of the healing process of skin lesion between diabetes and AD, KRAS could be used as a target for skin lesion healing in AD.

Interleukin 13 (IL13) participates in cutaneous Th2 related immune response and induce IL5 expression and eosinophil penetration. The clinical breast milk sample collected from mothers of 25 infants with AD and 26 healthy controls indicated IL13 producing cells in breast milk could be a potential biomarker for infantile AD diagnosis [24]. The clinical trials for tralokinumab and lebrikizumab are shown promising results for moderate-severe AD management [25].

Janus kinase 1 (JAK1) and Janus kinase 2 (JAK2) are the two members of the Janus kinase family which also includes Janus kinase 3 (JAK3) and Tyrosine kinase 2 (TYK2). JAK1 and JAK2 could modulate the AD-related cytokine production which involves in acute and chronic phase. Specifically, JAK1 could modulate pathways of cytokine including interleukin 4 (IL4), interleukin 6 (IL6), interleukin 10 (IL10), and interferon γ (IFNγ) in acute AD; JAK2 could modulate pathways of cytokine including interleukin 5 (IL5), interleukin 6 (IL6), interleukin 23 (IL23), IFNγ, and granulocyte-macrophage-colony-stimulating factor (GM-CSF) in acute AD and interleukin 12 (IL12) in chronic AD [26].

Signal transducer and activator of transcription 3 (STAT3) is indispensable for Th2 cytokine production and transcription factor expression. More importantly, STAT3 was proved to correlate with SCORAD index in childhood AD from 30 AD children and 28 healthy control group. Therefore, STAT3 could be used as a biomarker to demonstrate the severity of AD [27].

Interleukin 2 (IL2) is one of the cytokines which correlated with chronic pruritus and immune response. IL2 involved in the activation and proliferation of T lymphocytes and B lymphocytes, activation-induced cell death of T lymphocytes, and the elimination of self-reactive cells. Oclacitinib targeted IL2 to represent as a new therapeutic agent on the horizon for atopic itchiness and AD management [28,29].

Interleukin 4 receptor (IL4R) is associated with binding of interleukin 4 (IL4) and interleukin 13 (IL13) which regulate the IgE production and Th2 related cytokines. Clinically, Dupilumab approved by FDA is the new line of medication by target this protein for moderate to severe AD management [30].

Interleukin 21 (IL21) and interleukin 21 receptor (IL21R) had been found upregulated in the skin lesion from active AD patients but not in control group. The expression of IL21 and IL21R occurs in dermis infiltrating mononuclear leukocytes, and epidermal keratinocytes and along the dermal-epidermal junction, respectively. It is also observed that the lack of IL21 signaling leads to sensitization, T cell recruitment and expansion, and subsequent inflammation initiation dysfunction [31].

REL proto-oncogene, NF-kB subunit or (c-Rel) is nuclear translocation of the NF-κB transcription factors which associated with decreasing Th1 cytokine production and reduced proliferative responses of isolated T cells collected from patients with severe AD [32, 33]. RELB proto-oncogene, NF-kB subunit (RELB) deficiency animal model has similar skin lesions to human AD in following aspects which include infiltrating CD4$^+$ T cells and eosinophils in the skin, boosted the number of eosinophils in the blood and IgE in serum [34].

Via scratch wound healing assay, Platelet Derived Growth Factor Receptor Beta (PDGFRB) is strongly associated with the migration of fibroblasts into the scratched wound [35]. Thus, PDGFRB could be a useful protein for the recovery of skin wound from scratching in AD.

Forkhead box P3 (FOXP3) is deemed as one of the best markers for T-regulatory cells in AD. The imbalance between CD4$^+$ CD25^{high} T-regulatory cells and Th2 effector cells are viewed as the immunologic and inflammatory pathways for AD development. It is observed that the gene expression of FOXP3 was suppressed *in 20 active AD patients and elevated after narrowband-ultraviolet B intervention in comparison with 20 healthy controls [36].*

FDA approved medication Alitretinoin can bind with retinoic acid receptor alpha or RARA to exert the therapeutic effect on atopic hand dermatitis. It could reduce Th2 and Th17 cells correlated atopic response and boost FOXP3$^+$ cells by T cells immunosuppression and proinflammation reductions [37].

Epidermal growth factor receptor (EGFR) inhibited inflammation and EGFR inhibitors deteriorated S.aureus colonization on AD skin lesions. As a therapeutic target, EGFR signaling could be attributed for acute wound healing which contains early recruitment of neutrophils and ultimately the reconstruction of the physical barrier [38].

MYC proto-oncogene, bHLH transcription factor (MYC) have the genetic association with AD [20]. MYC is a transcription factor that binds DNA in a non-specific manner, yet also specifically recognizes the core sequence 5′-CAC[GA]TG-3′ which activates the transcription of growth-related genes. Binds to the vascular endothelial growth factor A (VEGFA promoter, promoting VEGFA production and subsequent producing angiogenesis [39,40].

Nuclear receptor subfamily 3 group C member 1 (NR3C1) which is also known as the glucocorticoid receptor (GR) exerts synthetic effect with peroxisome proliferator-activated receptors (PPARs) for anti-inflammatory effects in AD [41]. Currently, a vast number of medications are targeting GR as therapeutic agents for AD management such as prednisolone, Fluticasone propionate, Prednisolone, etc [42].

*From literature and ELSEVIER Pathway Studio (**Appendix**), some of the identified key targets could be associated with a specific phase or symptom of AD. Specifically, JAK1, JAK2, and CREBBP were correlated with pruritus; IL13 could be attributed to the acute phase of AD (Zhong, Liu, Zhou, & Xu, 2017).*

5. Conclusions

Taken together, the top 200 protein genes acquired from Open Targets Platform and later integrated analysis led to the identification of 173 genes nodes and 981 edges in a PPI network. Then, the top 50 hub genes were selected by five algorism methods from CytoHubba application. After the integrated genes process from intensive analysis of five algorism methods, it is obtained the elucidation of the 23 key hub genes (VDR, KIT, BCL2L11, NFKBIA, KRAS, IL13, JAK2, STAT3, IL21, IL4R, REL, PDGFRB, FOXP3, RARA, RELB, EGFR, IL21R, MYC, CREBBP, NR3C1, IL2, JAK1, and KITLG). They had been further enriched by ClueGo and CluePedia application to acquire major signaling pathways which were mainly correlated with JAK-STAT signaling pathway, Interleukin-21-mediated signaling pathway, and Interleukin-2 family signaling. These findings could dramatically better our understanding of the target proteins for AD medication discovery and diagnostic biomarker exploration. These key hub genes and key pathways could be further tested by our upcoming research to understand their interactions with natural compounds from traditional Chinese Medicinal herbs.

Supplementary Materials:

297 Supplement table 1. the target proteins for AD extracted from Open Targets Platform

Target gene info symbol	target. id	Association score . overall	Association score datatypes genetic association	Association Score datatypes somatic mutation	Association score datatypes known drug	Association score datatypes affected pathway	Association score datatypes RNA expression	Association score datatypes literature	Association score datatypes animal model	target.gene_info.name
IL13	ENSG00000169194	1	0.767367	0	1	0	0	0.088899	0	interleukin 13
FLG	ENSG00000143631	1	1	0	0	0	0.047899	0.168916	0.283556	filaggrin
IL4R	ENSG00000077238	1	0	0	1	0	0.010111	0.043034	0.272222	interleukin 4 receptor
RXRA	ENSG00000186350	1	0	0	1	0	0	0	0.228825	retinoid X receptor alpha
SPINK5	ENSG00000133710	1	1	0	0	0	0.010251	0.070368	0.18868	serine peptidase inhibitor, Kazal type 5
JAK2	ENSG00000096968	1	0	0	1	0	0.029453	0.034944	0.18306	Janus kinase 2
PPIA	ENS	1	0	0	1	0	0	0	0.2	peptidylprolyl isomerase A

	G00000196262									
FKBP1A	ENSG00000088832	1	0	0	1	0	0.017267	0	0.18306	FKBP prolyl isomerase 1A
NR3C1	ENSG00000113580	1	0	0	1	0	0.047175	0.041852	0	nuclear receptor subfamily 3 group C member 1
CD2	ENSG00000116824	1	0	0	1	0	0	0.052169	0	CD2 molecule
JAK1	ENSG00000162434	1	0	0	1	0	0.013488	0.042933	0	Janus kinase 1
VDR	ENSG00000111424	1	0	0	1	0	0	0.036622	0	vitamin D receptor
HRH1	ENSG00000196639	1	0	0	1	0	0	0.030442	0	histamine receptor H1
CYSLTR1	ENSG00000173198	1	0	0	1	0	0	0.0288	0	cysteinyl leukotriene receptor 1
PLA2G7	ENSG000	1	1	0	0	0	0.004216	0	0	phospholipase A2 group VII

	00146070									
IGHE	ENSG00000211891	1	0	0	1	0	0	0	0	immunoglobulin heavy constant epsilon
RXRB	ENSG00000204231	1	0	0	1	0	0	0	0	retinoid X receptor beta
PDE4B	ENSG00000184588	1	0	0	1	0	0	0	0	phosphodiesterase 4B
RARG	ENSG00000172819	1	0	0	1	0	0	0	0	retinoic acid receptor gamma
RXRG	ENSG00000143171	1	0	0	1	0	0	0	0	retinoid X receptor gamma
RARA	ENSG00000131759	1	0	0	1	0	0	0	0	retinoic acid receptor alpha
PDE4D	ENSG00000113448	1	0	0	1	0	0	0	0	phosphodiesterase 4D
PDE4C	ENSG0000010	1	0	0	1	0	0	0	0	phosphodiesterase 4C

	5650									
RARB	ENSG00000077092	1	0	0	1	0	0	0	0	retinoic acid receptor beta
PDE4A	ENSG00000065989	1	0	0	1	0	0	0	0	phosphodiesterase 4A
OVOL1	ENSG00000172818	0.892065	0.881273	0	0	0	0	0.043171	0	ovo like transcriptional repressor 1
TRPV1	ENSG00000196689	0.803025	0	0	0.782472	0	0.05041	0.059807	0	transient receptor potential cation channel subfamily V member 1
TACR1	ENSG00000115353	0.785031	0	0	0.772222	0	0	0.051233	0	tachykinin receptor 1
IL18R1	ENSG00000115604	0.780339	0.776739	0	0	0	0	0.0144	0	interleukin 18 receptor 1
AP5B1	ENSG00000254470	0.771769	0.771769	0	0	0	0	0	0	adaptor related protein complex 5 subunit beta 1
DHFR	ENSG00000228716	0.745765	0	0	0.7	0	0	0	0.18306	dihydrofolate reductase

PPP2R3C	ENSG00000092020	0.734951	0.734951	0	0	0	0	0	0	protein phosphatase 2 regulatory subunit B"gamma
LCE5A	ENSG00000186207	0.727624	0.727624	0	0	0	0	0	0	late cornified envelope 5A
HLA-B	ENSG00000234745	0.7261	0.7261	0	0	0	0	0	0	major histocompatibility complex, class I, B
LCE3E	ENSG00000185966	0.725	0.725	0	0	0	0	0	0	late cornified envelope 3E
ZNF365	ENSG00000138311	0.715	0.715	0	0	0	0	0	0	zinc finger protein 365
PRKRA	ENSG00000180228	0.7036	0.7	0	0	0	0	0.0144	0	protein activator of interferon induced protein kinase EIF2AK2
RASIP1	ENSG00000105538	0.695765	0.65	0	0	0	0	0	0.18306	Ras interacting protein 1
LRRC32	ENSG00000137507	0.694425	0.686625	0	0	0	0	0.0312	0	leucine rich repeat containing 32
TNX	ENS	0.66	0.666136	0	0	0	0	0	0	tenascin XB

B	G00000168477	6136								
PBX2	ENSG00000204304	0.665229	0.665229	0	0	0	0	0	0	PBX homeobox 2
KIF3A	ENSG00000131437	0.656606	0.647106	0	0	0	0	0.038	0	kinesin family member 3A
GLB1	ENSG00000170266	0.6553	0.65	0	0	0	0	0.0212	0	galactosidase beta 1
RAD50	ENSG00000113522	0.6519	0.65	0	0	0	0	0.0076	0	RAD50 double strand break repair protein
AC116366.3	ENSG00000283782	0.65	0.65	0	0	0	0	0	0	novel protein
TSBP1	ENSG00000204296	0.65	0.65	0	0	0	0	0	0	testis expressed basic protein 1
ZBTB10	ENSG00000205189	0.647222	0.647222	0	0	0	0	0	0	zinc finger and BTB domain containing 10
IL7R	ENSG000	0.64078	0.637905	0	0	0	0.011509	0	0	interleukin 7 receptor

	00168685	2								
ETS1	ENSG00000134954	0.625	0.625	0	0	0	0	0	0	ETS proto-oncogene 1, transcription factor
RTEL1	ENSG00000258366	0.623251	0.620951	0	0	0	0	0.0092	0	regulator of telomere elongation helicase 1
LCE1E	ENSG00000186226	0.616684	0.6	0	0	0	0.066736	0	0	late cornified envelope 1E
ANXA6	ENSG00000197043	0.610975	0.6	0	0	0	0	0.0439	0	annexin A6
CLEC16A	ENSG00000038532	0.512561	0.512561	0	0	0	0	0	0	C-type lectin domain containing 16A
CCDC80	ENSG00000091986	0.509678	0.5	0	0	0	0.032313	0.0144	0	coiled-coil domain containing 80
RPTN	ENSG00000215853	0.5077	0.5	0	0	0	0	0.0308	0	repetin
ACTL9	ENSG0000018	0.505337	0.496062	0	0	0	0	0.0371	0	actin like 9

	1786									
OR10A3	ENSG00000170683	0.504375	0.5	0	0	0	0	0.0175	0	olfactory receptor family 10 subfamily A member 3
SPRR1B	ENSG00000169469	0.491921	0.489966	0	0	0	0.007819	0	0	small proline rich protein 1B
KCNJ11	ENSG00000187486	0.49	0.49	0	0	0	0	0	0	potassium voltage-gated channel subfamily J member 11
IL6R	ENSG00000160712	0.441148	0.434048	0	0	0	0	0.0284	0	interleukin 6 receptor
IL18RAP	ENSG00000115607	0.427351	0.423299	0	0	0	0.00407	0.0144	0	interleukin 18 receptor accessory protein
PTPRN2	ENSG00000155093	0.412658	0.412658	0	0	0	0	0	0	protein tyrosine phosphatase receptor type N2
MRPS21	ENSG00000266472	0.402041	0.402041	0	0	0	0	0	0	mitochondrial ribosomal protein S21
TNFRSF6B	ENSG00000243509	0.397799	0.394199	0	0	0	0	0.0144	0	TNF receptor superfamily member 6b

STAT3	ENSG00000168610	0.397694	0.385817	0	0	0	0.006473	0.04463	0	signal transducer and activator of transcription 3
HRNR	ENSG00000197915	0.396218	0.384096	0	0	0	0	0.04849	0	hornerin
IL15RA	ENSG00000134470	0.380825	0.380825	0	0	0	0	0	0	interleukin 15 receptor subunit alpha
IKZF3	ENSG00000161405	0.366378	0.316378	0	0	0	0	0	0.2	IKAROS family zinc finger 3
XIRP2	ENSG00000163092	0.366342	0.320577	0	0	0	0	0	0.18306	xin actin binding repeat containing 2
KIAA1109	ENSG00000138688	0.364098	0.318333	0	0	0	0	0	0.18306	KIAA1109
DNAJB6	ENSG00000105993	0.335229	0.317429	0	0	0	0	0.0712	0	DnaJ heat shock protein family (Hsp40) member B6
EFHC1	ENSG00000096093	0.333622	0.333622	0	0	0	0	0	0	EF-hand domain containing 1
REL	ENS	0.32	0.326196	0	0	0	0	0	0	REL proto-oncogene, NF-kB

	G00000162924	6196								subunit
CARD11	ENSG00000198286	0.324261	0.269897	0	0	0	0	0.039277	0.2	caspase recruitment domain family member 11
VAX2	ENSG00000116035	0.324017	0.324017	0	0	0	0	0	0	ventral anterior homeobox 2
PRR5L	ENSG00000135362	0.323722	0.323722	0	0	0	0	0	0	proline rich 5 like
FOXC1	ENSG00000054598	0.313265	0.313265	0	0	0	0	0	0	forkhead box C1
MYT1L	ENSG00000186487	0.312947	0.312947	0	0	0	0	0	0	myelin transcription factor 1 like
PUS10	ENSG00000162927	0.312947	0.312947	0	0	0	0	0	0	pseudouridine synthase 10
FOXP3	ENSG00000049768	0.310548	0	0	0	0	0	0.073517	0.292169	forkhead box P3
ZGLP1	ENSG000	0.30753	0.307533	0	0	0	0	0	0	zinc finger GATA like protein 1

	00220201	3								
RNF111	ENSG00000157450	0.303333	0.303333	0	0	0	0	0	0	ring finger protein 111
IL21	ENSG00000138684	0.300453	0.244983	0	0	0	0	0.049231	0.2	interleukin 21
TRAF3IP2	ENSG00000056972	0.298278	0	0	0	0	0	0	0.298278	TRAF3 interacting protein 2
FCER2	ENSG00000104921	0.291941	0	0	0	0	0	0.078874	0.272222	Fc fragment of IgE receptor II
NFKBIZ	ENSG00000144802	0.289238	0	0	0	0	0	0.0192	0.284438	NFKB inhibitor zeta
ITGB2	ENSG00000160255	0.287772	0	0	0	0	0	0.0217	0.282347	integrin subunit beta 2
IL21R	ENSG00000103522	0.284722	0	0	0	0	0	0	0.284722	interleukin 21 receptor
CEBPE	ENSG0000009	0.284049	0	0	0	0	0	0	0.284049	CCAAT enhancer binding protein epsilon

	2067									
CTSE	ENSG00000196188	0.282655	0	0	0	0	0	0.046761	0.270964	cathepsin E
PTPN22	ENSG00000134242	0.281022	0	0	0	0	0	0.0352	0.272222	protein tyrosine phosphatase non-receptor type 22
GBA	ENSG00000177628	0.278407	0	0	0	0	0	0.0208	0.273207	glucosylceramidase beta
CHST8	ENSG00000124302	0.277244	0.277244	0	0	0	0	0	0	carbohydrate sulfotransferase 8
HLA-DRB1	ENSG00000196126	0.276701	0.276701	0	0	0	0	0	0	major histocompatibility complex, class II, DR beta 1
SLC6A15	ENSG00000072041	0.276701	0.276701	0	0	0	0	0	0	solute carrier family 6 member 15
MGMT	ENSG00000170430	0.275513	0.269613	0	0	0	0	0.0236	0	O-6-methylguanine-DNA methyltransferase
DSG3	ENSG00000134757	0.274317	0	0	0	0	0.01075	0	0.27163	desmoglein 3

TNIP1	ENSG00000145901	0.27394	0	0	0	0	0	0.0144	0.27034	TNFAIP3 interacting protein 1
NFKBIA	ENSG00000100906	0.273796	0	0	0	0	0	0.016	0.269796	NFKB inhibitor alpha
KITLG	ENSG00000049130	0.272978	0	0	0	0	0	0.049485	0.260606	KIT ligand
NTRK1	ENSG00000198400	0.272447	0	0	0.261111	0	0	0.045344	0	neurotrophic receptor tyrosine kinase 1
LAT	ENSG00000213658	0.272222	0	0	0	0	0	0	0.272222	linker for activation of T cells
SLC4A1	ENSG00000004939	0.267929	0	0	0	0	0	0	0.267929	solute carrier family 4 member 1 (Diego blood group)
DMRTA1	ENSG00000176399	0.266667	0.266667	0	0	0	0	0	0	DMRT like family A1
IL1R1	ENSG00000115594	0.266283	0.261983	0	0	0	0	0.0172	0	interleukin 1 receptor type 1
KIT	ENS	0.26	0	0	0	0	0	0	0.266226	KIT proto-oncogene,

	G00000157404	6226									receptor tyrosine kinase
SCD	ENSG00000099194	0.265676	0	0	0	0	0	0.0104	0.263076	stearoyl-CoA desaturase
PTGDR2	ENSG00000183134	0.265366	0	0	0.25	0	0	0.061466	0	prostaglandin D2 receptor 2
CHD7	ENSG00000171316	0.265259	0	0	0	0	0	0	0.265259	chromodomain helicase DNA binding protein 7
IL17A	ENSG00000112115	0.263189	0	0	0.25	0	0	0.052758	0	interleukin 17A
FASLG	ENSG00000117560	0.261487	0	0	0	0	0	0.045948	0.25	Fas ligand
EGFR	ENSG00000146648	0.261452	0	0	0	0	0.042764	0.042665	0.24602	epidermal growth factor receptor
CYP24A1	ENSG00000019186	0.260607	0.256632	0	0	0	0	0.0159	0	cytochrome P450 family 24 subfamily A member 1
MEIS1	ENSG000	0.26060	0	0	0	0	0	0	0.260606	Meis homeobox 1

	00143995	6								
MFN2	ENSG00000116688	0.26	0.26	0	0	0	0	0	0	mitofusin 2
IL12B	ENSG00000113302	0.2574	0	0	0.25	0	0	0.0296	0	interleukin 12B
STK36	ENSG00000163482	0.256576	0	0	0	0	0.030182	0	0.24903	serine/threonine kinase 36
MMP1	ENSG00000196611	0.2554331	0	0	0.25	0	0.021725	0	0	matrix metallopeptidase 1
RELB	ENSG00000104856	0.2550177	0	0	0	0	0.007626	0.028	0.24717	RELB proto-oncogene, NF-kB subunit
TBL1XR1	ENSG00000177565	0.254736	0.246598	0	0	0	0.032553	0	0	transducin beta like 1 X-linked receptor 1
ITK	ENSG00000113263	0.2542	0	0	0	0	0.004053	0.015	0.25	IL2 inducible T cell kinase
ZAP70	ENSG0000011	0.2541	0	0	0	0	0	0.0164	0.25	zeta chain of T cell receptor associated protein kinase 70

	5085									
JAK3	ENSG00000105639	0.254015	0	0	0.2	0	0.006823	0.0323	0.2	Janus kinase 3
F3	ENSG00000117525	0.253495	0	0	0	0	0.017322	0	0.249165	coagulation factor III, tissue factor
RASGRP1	ENSG00000172575	0.251969	0	0	0	0	0.007877	0	0.25	RAS guanyl releasing protein 1
STK4	ENSG00000101109	0.251965	0	0	0	0	0.007858	0	0.25	serine/threonine kinase 4
TSLP	ENSG00000145777	0.251869	0	0	0.225	0	0	0.107478	0	thymic stromal lymphopoietin
GPC3	ENSG00000147257	0.251472	0	0	0	0	0.00977	0	0.24903	glypican 3
MMP7	ENSG00000137673	0.251165	0	0	0.25	0	0.00466	0	0	matrix metallopeptidase 7
LYN	ENSG00000254087	0.25	0	0	0	0	0	0	0.25	LYN proto-oncogene, Src family tyrosine kinase

MMP13	ENSG00000137745	0.25	0	0	0.25	0	0	0	0	matrix metallopeptidase 13
MMP8	ENSG00000118113	0.25	0	0	0.25	0	0	0	0	matrix metallopeptidase 8
WAS	ENSG00000015285	0.25	0	0	0	0	0	0	0.25	WASP actin nucleation promoting factor
IL6ST	ENSG00000134352	0.24959	0	0	0	0	0	0	0.24959	interleukin 6 signal transducer
SPTA1	ENSG00000163554	0.249165	0	0	0	0	0	0	0.249165	spectrin alpha, erythrocytic 1
NSDHL	ENSG00000147383	0.249165	0	0	0	0	0	0	0.249165	NAD(P) dependent steroid dehydrogenase-like
RB1	ENSG00000139687	0.249165	0	0	0	0	0	0	0.249165	RB transcriptional corepressor 1
TTC7A	ENSG00000068724	0.249165	0	0	0	0	0	0	0.249165	tetratricopeptide repeat domain 7A
CUX	ENS	0.24	0	0	0	0	0	0	0.24903	cut like homeobox 1

1	G00000257923	903									
E2F4	ENSG00000205250	0.24903	0	0	0	0	0	0	0.24903	E2F transcription factor 4
HYDIN	ENSG00000157423	0.24903	0	0	0	0	0	0	0.24903	HYDIN axonemal central pair apparatus protein
AK7	ENSG00000140057	0.24903	0	0	0	0	0	0	0.24903	adenylate kinase 7
TTLL1	ENSG00000100271	0.24903	0	0	0	0	0	0	0.24903	tubulin tyrosine ligase like 1
TP73	ENSG00000078900	0.24903	0	0	0	0	0	0	0.24903	tumor protein p73
CACNA2D2	ENSG00000007402	0.24903	0	0	0	0	0	0	0.24903	calcium voltage-gated channel auxiliary subunit alpha2delta 2
DSG4	ENSG00000175065	0.24717	0	0	0	0	0	0	0.24717	desmoglein 4
PSTPIP2	ENSG000	0.24717	0	0	0	0	0	0	0.24717	proline-serine-threonine phosphatase interacting

	00152229									protein 2
COL8A2	ENSG00000171812	0.247125	0	0	0	0	0	0	0.247125	collagen type VIII alpha 2 chain
MICB	ENSG00000204516	0.246955	0.246955	0	0	0	0	0	0	MHC class I polypeptide-related sequence B
DDX39B	ENSG00000198563	0.246955	0.246955	0	0	0	0	0	0	DExD-box helicase 39B
ID2	ENSG00000115738	0.246598	0.246598	0	0	0	0	0	0	inhibitor of DNA binding 2
KRT10	ENSG00000186395	0.243875	0	0	0	0	0	0.0321	0.23585	keratin 10
LUM	ENSG00000139329	0.24379	0	0	0	0	0	0	0.24379	lumican
ALOX12B	ENSG00000179477	0.242115	0	0	0	0	0.00666	0	0.24045	arachidonate 12-lipoxygenase, 12R type
KRAS	ENSG0000013	0.239421	0	0	0	0	0.042386	0	0.228825	KRAS proto-oncogene, GTPase

	3703									
SMARCA4	ENSG00000127616	0.239325	0.239325	0	0	0	0	0	0	SWI/SNF related, matrix associated, actin dependent regulator of chromatin, subfamily a, member 4
GRM4	ENSG00000124493	0.239325	0.239325	0	0	0	0	0	0	glutamate metabotropic receptor 4
ST14	ENSG00000149418	0.239045	0	0	0	0	0	0	0.239045	suppression of tumorigenicity 14
MPZL3	ENSG00000160588	0.237275	0	0	0	0	0	0	0.237275	myelin protein zero like 3
RAF1	ENSG00000132155	0.234825	0	0	0	0	0	0.024	0.228825	Raf-1 proto-oncogene, serine/threonine kinase
NPM1	ENSG00000181163	0.234625	0	0	0	0	0	0.0232	0.228825	nucleophosmin 1
XPA	ENSG00000136936	0.234445	0	0	0	0	0	0	0.234445	XPA, DNA damage recognition and repair factor
CEP76	ENSG00000101624	0.233333	0.233333	0	0	0	0	0	0	centrosomal protein 76

TGM3	ENSG00000125780	0.231585	0.229711	0	0	0	0.007496	0	0	transglutaminase 3
COL5A2	ENSG00000204262	0.230125	0	0	0	0	0	0	0.230125	collagen type V alpha 2 chain
FST	ENSG00000134363	0.230068	0	0	0	0	0.004971	0	0.228825	follistatin
PBX1	ENSG00000185630	0.228825	0	0	0	0	0	0	0.228825	PBX homeobox 1
ZFPM1	ENSG00000179588	0.228825	0	0	0	0	0	0	0.228825	zinc finger protein, FOG family member 1
RAD9A	ENSG00000172613	0.228825	0	0	0	0	0	0	0.228825	RAD9 checkpoint clamp component A
ILK	ENSG00000166333	0.228825	0	0	0	0	0	0	0.228825	integrin linked kinase
ZNF148	ENSG00000163848	0.228825	0	0	0	0	0	0	0.228825	zinc finger protein 148
TAL1	ENS	0.22	0	0	0	0	0	0	0.228825	TAL bHLH transcription

	G00000162367	8825								factor 1, erythroid differentiation factor
NFE2	ENSG00000123405	0.228825	0	0	0	0	0	0	0.228825	nuclear factor, erythroid 2
ARAP3	ENSG00000120318	0.228825	0	0	0	0	0	0	0.228825	ArfGAP with RhoGAP domain, ankyrin repeat and PH domain 3
TCF21	ENSG00000118526	0.228825	0	0	0	0	0	0	0.228825	transcription factor 21
PDGFRB	ENSG00000113721	0.228825	0	0	0	0	0	0	0.228825	platelet derived growth factor receptor beta
SOD2	ENSG00000112096	0.228825	0	0	0	0	0	0	0.228825	superoxide dismutase 2
MAPK14	ENSG00000112062	0.228825	0	0	0	0	0	0	0.228825	mitogen-activated protein kinase 14
ATE1	ENSG00000107669	0.228825	0	0	0	0	0	0	0.228825	arginyltransferase 1
PIEZO1	ENSG000	0.22882	0	0	0	0	0	0	0.228825	piezo type mechanosensitive ion channel component 1

	00103335	5								
NPRL3	ENSG00000103148	0.228825	0	0	0	0	0	0	0.228825	NPR3 like, GATOR1 complex subunit
GATA1	ENSG00000102145	0.228825	0	0	0	0	0	0	0.228825	GATA binding protein 1
XBP1	ENSG00000100219	0.228825	0	0	0	0	0	0	0.228825	X-box binding protein 1
ELP1	ENSG00000070061	0.228825	0	0	0	0	0	0	0.228825	elongator complex protein 1
CREBBP	ENSG00000005339	0.228825	0	0	0	0	0	0	0.228825	CREB binding protein
KRIT1	ENSG00000001631	0.228825	0	0	0	0	0	0	0.228825	KRIT1 ankyrin repeat containing
NCF4	ENSG00000100365	0.22628	0.22628	0	0	0	0	0	0	neutrophil cytosolic factor 4
IFNG	ENSG0000011	0.225875	0	0	0	0	0	0.1035	0.2	interferon gamma

	1537									
ITGAL	ENSG00000005844	0.225	0	0	0.225	0	0	0	0	integrin subunit alpha L
IL10	ENSG00000136634	0.224236	0	0	0	0	0	0.096945	0.2	interleukin 10
R3HCC1L	ENSG00000166024	0.223379	0.223379	0	0	0	0	0	0	R3H domain and coiled-coil containing 1 like
CCR4	ENSG00000183813	0.223378	0	0	0	0	0	0.093512	0.2	C-C motif chemokine receptor 4
TMEM235	ENSG00000204278	0.223299	0.223299	0	0	0	0	0	0	transmembrane protein 235
MYC	ENSG00000136997	0.222014	0.213265	0	0	0	0.034996	0	0	MYC proto-oncogene, bHLH transcription factor
IL2	ENSG00000109471	0.221073	0	0	0	0	0	0.084292	0.2	interleukin 2
KPNA3	ENSG00000102753	0.218649	0.218649	0	0	0	0	0	0	karyopherin subunit alpha 3

RORA	ENSG00000069667	0.218628	0	0	0	0	0.068112	0.0144	0.2	RAR related orphan receptor A
TGFB1	ENSG00000105329	0.217524	0	0	0	0	0	0.076655	0.19836	transforming growth factor beta 1
IL22	ENSG00000127318	0.21746	0	0	0.2	0	0.00476	0.067724	0	interleukin 22
BCL2L11	ENSG00000153094	0.217429	0.217429	0	0	0	0	0	0	BCL2 like 11

Supplement table 2. Node table of 173 targets extracted from Cytoscape

SUID	Average Shortest Path Length	Betweenness Centrality	Closeness Centrality	Clustering Coefficient	Degree	Eccentricity	IsSingle Node	name	Neighbourhood Connectivity	Number of Directed Edges	Number of Undirected Edges	Partner of Multi Edged Node Pairs	Radiality	selected	Self-Loops	shared name	Stress	Topological Coefficient
237	1.889535	0.11139	0.529231	0.254363	62	4	FALSE	STAT3	20.59677	62	0	0	0.888808	FALSE	0	STAT3	21646	0.153587
225	1.953488	0.074307	0.511905	0.282581	57	5	FALSE	IL2	21.47368	57	0	0	0.880814	FALSE	0	IL2	17498	0.161456
240	1.953488	0.087913	0.511905	0.247138	55	4	FALSE	EGFR	21.16364	55	0	0	0.880814	FALSE	0	EGFR	20780	0.160193

223	1.965116	0.067256	0.508876	0.301188	54	5	FALSE	IL10	22.07407	54	0	0	0.87936	FALSE	0	IL10	15416	0.16597
204	1.918605	0.126623	0.521212	0.235294	52	4	FALSE	MYC	20.15385	52	0	0	0.885174	FALSE	0	MYC	24162	0.146828
211	2.023256	0.056931	0.494253	0.314976	46	5	FALSE	IL17A	22.08696	46	0	0	0.872093	FALSE	0	IL17A	12790	0.1699
226	2.104651	0.020716	0.475138	0.387179	40	5	FALSE	FOXP3	25.1	40	0	0	0.861919	FALSE	0	FOXP3	7142	0.199206
201	2.122093	0.027087	0.471233	0.438122	38	5	FALSE	IFNG	26.18421	38	0	0	0.859738	FALSE	0	IFNG	7700	0.211163
235	2.139535	0.038397	0.467391	0.40991	37	5	FALSE	IL13	24.32432	37	0	0	0.857558	FALSE	0	IL13	9688	0.19938
238	2.127907	0.017677	0.469945	0.462185	35	5	FALSE	JAK2	27.8	35	0	0	0.859012	FALSE	0	JAK2	5710	0.222171
221	2.215116	0.023934	0.451444	0.424242	34	5	FALSE	IL7R	25.47059	34	0	0	0.84811	FALSE	0	IL7R	7134	0.221483
190	2.145349	0.035591	0.466125	0.334677	32	5	FALSE	MAPK14	25.1875	32	0	0	0.856831	FALSE	0	MAPK14	8886	0.197835
208	2.156977	0.059746	0.463612	0.289655	30	4	FALSE	CREBBP	19.96667	30	0	0	0.855378	FALSE	0	CREBBP	1181	0.159467

																	0	
239	2.180233	0.021288	0.458667	0.344828	30	4	FALSE	KRAS	24.3	30	0	0	0.852471	FALSE	0	KRAS	6490	0.200551
189	2.174419	0.045431	0.459893	0.306878	28	5	FALSE	LYN	23.28571	28	0	0	0.853198	FALSE	0	LYN	10626	0.189024
212	2.238372	0.004965	0.446753	0.592593	28	5	FALSE	JAK3	30.28571	28	0	0	0.845203	FALSE	0	JAK3	2086	0.263354
227	2.25	0.003094	0.444444	0.635328	27	5	FALSE	JAK1	31.03704	27	0	0	0.84375	FALSE	0	JAK1	1476	0.272255
202	2.226744	0.037232	0.449086	0.525362	24	4	FALSE	PDGFRB	30.29167	24	0	0	0.846657	FALSE	0	PDGFRB	7730	0.254552
231	2.354651	0.004967	0.424691	0.561594	24	5	FALSE	IL21	28.5	24	0	0	0.830669	FALSE	0	IL21	1196	0.274038
242	2.215116	0.013745	0.451444	0.478261	24	5	FALSE	KIT	29.625	24	0	0	0.84811	FALSE	0	KIT	4714	0.238911
176	2.244186	0.010729	0.445596	0.43083	23	5	FALSE	ETS1	29.30435	23	0	0	0.844477	FALSE	0	ETS1	3920	0.244203
183	2.232558	0.024617	0.447917	0.418972	23	5	FALSE	TGFB1	28.34783	23	0	0	0.84593	FALSE	0	TGFB1	5298	0.23587
214	2.244186	0.012124	0.445596	0.470356	23	5	FALSE	ZAP70	28.43478	23	0	0	0.844477	FALSE	0	ZAP70	4504	0.236957
1	2.30814	0.00724	0.4332	0.69697	22	5	FAL	IL22	31.54545	22	0	0	0.8	F	0	IL22	2	0.28

96		3	49				SE						36483	ALSE			802	6777
222	2.273256	0.011963	0.439898	0.679654	22	5	FALSE	TSLP	31.54545	22	0	0	0.840843	FALSE	0	TSLP	4504	0.276715
228	2.284884	0.02081	0.437659	0.419913	22	5	FALSE	NFKBIA	27.27273	22	0	0	0.83939	FALSE	0	NFKBIA	5024	0.236759
220	2.389535	0.036849	0.418491	0.285714	21	5	FALSE	GATA1	17.61905	21	0	0	0.826308	FALSE	0	GATA1	8872	0.172736
232	2.412791	0.001982	0.414458	0.652381	21	5	FALSE	IL21R	30.28571	21	0	0	0.823401	FALSE	0	IL21R	830	0.309038
236	2.406977	5.49E-04	0.415459	0.761905	21	5	FALSE	IL4R	31.57143	21	0	0	0.824128	FALSE	0	IL4R	270	0.315714
209	2.453488	3.06E-04	0.407583	0.815789	20	5	FALSE	IL6R	32.55	20	0	0	0.818314	FALSE	0	IL6R	134	0.339063
233	2.343023	0.015476	0.426799	0.363158	20	5	FALSE	RARA	21.55	20	0	0	0.832122	FALSE	0	RARA	4520	0.202358
173	2.261628	0.020033	0.442159	0.467836	19	5	FALSE	FASLG	31.10526	19	0	0	0.842297	FALSE	0	FASLG	4804	0.267241
182	2.302326	0.033393	0.434343	0.397661	19	4	FALSE	VDR	26.89474	19	0	0	0.837209	FALSE	0	VDR	6900	0.239662
203	2.389535	0.016522	0.418491	0.345029	19	5	FALSE	PTPN22	23.63158	19	0	0	0.826308	FALSE	0	PTPN22	4600	0.23065

241	2.279077	0.007027	0.438776	0.526316	19	5	FALSE	KITLG	32.21053	19	0	0	0.840116	FALSE	0	KITLG	2598	0.275304
181	2.424419	0.091765	0.41247	0.169935	18	5	FALSE	FLG	12.83333	18	0	0	0.821948	FALSE	0	FLG	18828	0.13173
186	2.372093	0.001284	0.421569	0.712418	18	5	FALSE	IL12B	33.5	18	0	0	0.828488	FALSE	0	IL12B	562	0.313084
187	2.406977	8.88E-04	0.415459	0.699346	18	5	FALSE	IL1R1	32.22222	18	0	0	0.824128	FALSE	0	IL1R1	448	0.315904
191	2.244186	0.010717	0.445596	0.48366	18	4	FALSE	NR3C1	29.38889	18	0	0	0.844477	FALSE	0	NR3C1	3094	0.237007
244	2.348837	0.009995	0.425743	0.333333	18	5	FALSE	ITGB2	23.05556	18	0	0	0.831395	FALSE	0	ITGB2	2606	0.211519
185	2.319767	0.004975	0.431078	0.544118	17	5	FALSE	MMP1	30.29412	17	0	0	0.835029	FALSE	0	MMP1	1794	0.265738
217	2.377907	0.014995	0.420538	0.360294	17	5	FALSE	RB1	21.52941	17	0	0	0.827762	FALSE	0	RB1	3102	0.205882
134	2.494186	0.002812	0.400932	0.558333	16	6	FALSE	CD2	27.75	16	0	0	0.813227	FALSE	0	CD2	956	0.304945
170	2.377907	0.01644	0.420538	0.491667	16	5	FALSE	BCL2L11	31.125	16	0	0	0.827762	FALSE	0	BCL2L11	3782	0.284977
19	2.540698	0.004823	0.393593	0.45	16	5	FALSE	ITK	22.625	16	0	0	0.807	FA	0	ITK	13	0.24260

3													413	LSE			22	8
207	2.511628	1.50E-04	0.398148	0.825	16	5	FALSE	IL6ST	31.375	16	0	0	0.811047	FALSE	0	IL6ST	70	0.348611
229	2.354651	0.004916	0.424691	0.558333	16	5	FALSE	REL	32.0625	16	0	0	0.830669	FALSE	0	REL	1876	0.288851
230	2.593023	0.006466	0.38565	0.441667	16	5	FALSE	RXRA	16.25	16	0	0	0.800872	FALSE	0	RXRA	1462	0.216667
172	2.412791	0.002741	0.414458	0.580952	15	5	FALSE	RELB	30.13333	15	0	0	0.823401	FALSE	0	RELB	1184	0.289744
192	2.540698	0.027845	0.393593	0.333333	15	6	FALSE	HLA-DRB1	22.66667	15	0	0	0.807413	FALSE	0	HLA-DRB1	6348	0.259004
197	2.366279	0.033344	0.422604	0.447619	15	5	FALSE	SMARCA4	23.8	15	0	0	0.829215	FALSE	0	SMARCA4	6850	0.223899
167	2.476744	0.008575	0.403756	0.448718	13	5	FALSE	WAS	21.53846	13	0	0	0.815407	FALSE	0	WAS	1726	0.225911
199	2.587209	0.023026	0.386517	0.410256	13	5	FALSE	MEIS1	18.07692	13	0	0	0.801599	FALSE	0	MEIS1	4558	0.226874
216	2.401163	0.003574	0.416465	0.551282	13	5	FALSE	RAF1	29.84615	13	0	0	0.824855	FALSE	0	RAF1	1238	0.273818
128	2.459302	0.003086	0.406619	0.545455	12	5	FALSE	NPM1	29.41667	12	0	0	0.817587	FALSE	0	NPM1	780	0.288399
1	2.48837	0.00343	0.4018	0.40909	12	5	FAL	CARD	23.41667	12	0	0	0.8	F	0	CARD	9	0.24

77	2	1	69	1			SE	11					13953	ALSE		11	82	3924
224	2.627907	0.002052	0.380531	0.606061	12	5	FALSE	RARG	18.91667	12	0	0	0.796512	FALSE	0	RARG	604	0.248904
243	2.569767	2.91E-04	0.38914	0.712121	12	6	FALSE	ITGAL	32.16667	12	0	0	0.803779	FALSE	0	ITGAL	120	0.369732
141	2.47093	9.95E-04	0.404706	0.745455	11	5	FALSE	MMP13	33.45455	11	0	0	0.816134	FALSE	0	MMP13	522	0.331233
161	2.44186	0.001029	0.409524	0.618182	11	5	FALSE	MMP7	34.27273	11	0	0	0.819767	FALSE	0	MMP7	374	0.332745
178	2.418605	0.001811	0.413462	0.527273	11	5	FALSE	ID2	33.63636	11	0	0	0.822674	FALSE	0	ID2	786	0.314359
200	2.639535	0.001515	0.378855	0.6	11	5	FALSE	PBX1	19.54545	11	0	0	0.795058	FALSE	0	PBX1	386	0.271465
213	2.703488	0.003328	0.369892	0.436364	11	5	FALSE	TAL1	17.36364	11	0	0	0.787064	FALSE	0	TAL1	1258	0.241162
206	2.517442	0.002122	0.397229	0.733333	10	5	FALSE	IL18R1	36	10	0	0	0.81032	FALSE	0	IL18R1	670	0.382979
210	2.767442	0.001316	0.361345	0.6	10	5	FALSE	RARB	16	10	0	0	0.77907	FALSE	0	RARB	310	0.262295
99	2.5	0.008163	0.4	0.583333	9	5	FALSE	SOD2	30.22222	9	0	0	0.8125	FALSE	0	SOD2	1762	0.307256

117	2.831395	0.017837	0.353183	0.166667	9	5	FALSE	ACTL9	7.555556	9	0	0	0.771076	FALSE	0	ACTL9	2150	0.146667
123	2.633721	0.022879	0.379691	0.194444	9	5	FALSE	ENSG00000196689	17.66667	9	0	0	0.795785	FALSE	0	ENSG00000196689	4426	0.216667
136	2.639535	0.017282	0.378855	0.444444	9	6	FALSE	PTGDR2	25.55556	9	0	0	0.795058	FALSE	0	PTGDR2	3324	0.314129
215	2.616279	0.001162	0.382222	0.666667	9	5	FALSE	LAT	25.66667	9	0	0	0.797965	FALSE	0	LAT	522	0.28839
234	2.924419	5.68E-04	0.341948	0.722222	9	5	FALSE	RXRB	13.66667	9	0	0	0.759448	FALSE	0	RXRB	2006	0.297101
165	2.674419	0.020854	0.373913	0.107143	8	5	FALSE	FKBP1A	14.5	8	0	0	0.790698	FALSE	0	FKBP1A	3196	0.18109
169	2.517442	0.010538	0.397229	0.535714	8	5	FALSE	GBA	32.875	8	0	0	0.81032	FALSE	0	GBA	1672	0.352151
171	3.267442	0.007702	0.30605	0.571429	8	6	FALSE	SPRR1B	7.125	8	0	0	0.71657	FALSE	0	SPRR1B	2822	0.323864
179	2.877907	0.01044	0.347475	0.464286	8	5	FALSE	RASGRP1	16.625	8	0	0	0.765262	FALSE	0	RASGRP1	3260	0.3
188	2.616279	1.32E-04	0.382222	0.821429	8	5	FALSE	IKZF3	35.375	8	0	0	0.797965	FALSE	0	IKZF3	78	0.406609
198	2.930233	1.96E-04	0.34127	0.857143	8	5	FALSE	RXRG	15.125	8	0	0	0.75872	FALS	0	RXRG	54	0.328804

													1	E				
107	2.656977	0.005109	0.376368	0.380952	7	5	FALSE	LRRC32	25.28571	7	0	0	0.792878	FALSE	0	LRRC32	1380	0.324176
115	2.598837	0.014466	0.384787	0.380952	7	5	FALSE	MGMT	26	7	0	0	0.800145	FALSE	0	MGMT	3670	0.304202
118	2.55814	0.039232	0.390909	0.190476	7	5	FALSE	OVOL1	14.14286	7	0	0	0.805233	FALSE	0	OVOL1	4880	0.16899
120	2.895349	0.014364	0.345382	0.238095	7	6	FALSE	CLEC16A	13	7	0	0	0.763081	FALSE	0	CLEC16A	3564	0.233766
126	2.755814	6.30E-04	0.362869	0.333333	7	5	FALSE	FOXC1	21.14286	7	0	0	0.780523	FALSE	0	FOXC1	224	0.285714
156	2.901163	0.003227	0.344689	0.238095	7	5	FALSE	LUM	14.57143	7	0	0	0.762355	FALSE	0	LUM	480	0.285714
166	3.284884	0.007397	0.304425	0.619048	7	6	FALSE	RPTN	7.428571	7	0	0	0.71439	FALSE	0	RPTN	2764	0.353742
184	2.610465	7.17E-04	0.383074	0.571429	7	5	FALSE	TP73	24.42857	7	0	0	0.798692	FALSE	0	TP73	238	0.313187
218	2.616279	5.38E-04	0.382222	0.619048	7	5	FALSE	E2F4	25	7	0	0	0.797965	FALSE	0	E2F4	148	0.297619
104	3.27907	0.015639	0.304965	0.133333	6	6	FALSE	OR10A3	4.5	6	0	0	0.715116	FALSE	0	OR10A3	1976	0.25
11	2.994186	7.38E-04	0.333981	0.333333	6	6	FALSE	TNIP1	16	6	0	0	0.750	FA	0	TNIP1	19	0.33333

3													727	LSE			6	3
127	2.598837	5.24E-05	0.384787	0.8	6	5	FALSE	ILK	36.66667	6	0	0	0.800145	FALSE	0	ILK	26	0.398551
130	2.912791	0.003856	0.343313	0.4	6	6	FALSE	SPINK5	14.5	6	0	0	0.760901	FALSE	0	SPINK5	1178	0.284314
133	2.732558	0.005777	0.365957	0.533333	6	5	FALSE	NFE2	20.33333	6	0	0	0.78343	FALSE	0	NFE2	1486	0.308081
137	2.802326	0.003078	0.356846	0.466667	6	6	FALSE	CCR4	28.16667	6	0	0	0.774709	FALSE	0	CCR4	644	0.402381
139	3.313953	0.004668	0.301754	0.4	6	6	FALSE	HRNR	7.5	6	0	0	0.710756	FALSE	0	HRNR	1458	0.318841
147	2.587209	0.001281	0.386517	0.733333	6	5	FALSE	CUX1	33.16667	6	0	0	0.801599	FALSE	0	CUX1	432	0.349123
148	2.843023	0.001281	0.351738	0.266667	6	5	FALSE	SPTA1	17.5	6	0	0	0.769622	FALSE	0	SPTA1	338	0.286111
158	2.662791	0	0.375546	1	6	5	FALSE	IL15RA	38.16667	6	0	0	0.792151	FALSE	0	IL15RA	0	0.465447
164	2.680233	0.014676	0.373102	0.466667	6	5	FALSE	DSG3	17.33333	6	0	0	0.789971	FALSE	0	DSG3	3046	0.225877
175	3.366279	0.004956	0.297064	0.733333	6	6	FALSE	LCE3E	8	6	0	0	0.704215	FALSE	0	LCE3E	2004	0.380952
2	2.91860	0.01207	0.3426	0.26666	6	6	FAL	IL18R	15.5	6	0	0	0.7	F	0	IL18R	2	0.27

05	5	2	29	7			SE	AP					60174	ALSE		AP	434	381
88	2.895349	0.004218	0.345382	0.3	5	6	FALSE	TGM3	13.4	5	0	0	0.763081	FALSE	0	TGM3	982	0.269388
92	2.662791	0.015192	0.375546	0.3	5	5	FALSE	XBP1	26.6	5	0	0	0.792151	FALSE	0	XBP1	2188	0.3275
94	2.598837	5.75E-06	0.384787	0.9	5	5	FALSE	MMP8	48.2	5	0	0	0.800145	FALSE	0	MMP8	6	0.541573
96	2.709302	0	0.369099	1	5	5	FALSE	NFKBIZ	32.2	5	0	0	0.786337	FALSE	0	NFKBIZ	0	0.429333
105	2.901163	0.004287	0.344689	0.2	5	5	FALSE	SLC4A1	16	5	0	0	0.762355	FALSE	0	SLC4A1	784	0.322449
121	3.063953	7.78E-04	0.326376	0.3	5	5	FALSE	CEBPE	13.8	5	0	0	0.742006	FALSE	0	CEBPE	246	0.331707
132	3.034884	0.010075	0.329502	0.2	5	6	FALSE	PDE4D	9.2	5	0	0	0.74564	FALSE	0	PDE4D	1958	0.225641
144	2.80814	6.60E-04	0.356108	0.7	5	5	FALSE	CYP24A1	19.6	5	0	0	0.773983	FALSE	0	CYP24A1	262	0.316129
149	2.796512	0.003378	0.357588	0.4	5	5	FALSE	TACR1	21	5	0	0	0.775436	FALSE	0	TACR1	888	0.291667
151	3.284884	1.59E-04	0.304425	0.7	5	6	FALSE	DSG4	8.8	5	0	0	0.71439	FALSE	0	DSG4	26	0.4

157	3.093023	0.024587	0.323308	0.1	5	5	FALSE	COL5A2	7.2	5	0	0	0.738372	FALSE	0	COL5A2	3808	0.22
160	2.622093	8.63E-04	0.381375	0.5	5	5	FALSE	NTRK1	34.4	5	0	0	0.797238	FALSE	0	NTRK1	360	0.402353
194	4.19186	1.40E-04	0.238558	0.8	5	7	FALSE	LCE5A	6.2	5	0	0	0.601017	FALSE	0	LCE5A	24	0.62
219	3.337209	1.77E-04	0.299652	0.5	5	6	FALSE	ZFPM1	9.2	5	0	0	0.707849	FALSE	0	ZFPM1	14	0.383333
90	2.773256	6.78E-05	0.360587	0.833333	4	6	FALSE	MICB	36.25	4	0	0	0.778343	FALSE	0	MICB	20	0.496575
111	3.726744	0.011865	0.268331	0.166667	4	7	FALSE	AK7	3	4	0	0	0.659157	FALSE	0	AK7	2198	0.416667
114	2.686047	8.83E-04	0.372294	0.5	4	5	FALSE	DHFR	30.5	4	0	0	0.789244	FALSE	0	DHFR	216	0.392857
116	2.848837	8.13E-04	0.35102	0	4	5	FALSE	PPIA	19	4	0	0	0.768895	FALSE	0	PPIA	130	0.321429
119	2.883721	1.78E-04	0.346774	0.833333	4	6	FALSE	TRAF3IP2	22.5	4	0	0	0.764535	FALSE	0	TRAF3IP2	110	0.401786
122	2.697674	0	0.37069	1	4	5	FALSE	F3	51	4	0	0	0.787791	FALSE	0	F3	0	0.614458
124	2.953488	9.48E-05	0.338583	0.5	4	6	FALSE	NCF4	19.75	4	0	0	0.75581	FALS	0	NCF4	40	0.397959

													4	E				
129	3.063953	0.001891	0.326376	0.333333	4	6	FALSE	KRT10	11	4	0	0	0.742006	FALSE	0	KRT10	414	0.325758
135	3.122093	0.01253	0.320298	0.166667	4	5	FALSE	KIF3A	8	4	0	0	0.734738	FALSE	0	KIF3A	1528	0.3125
143	2.813953	0.003352	0.355372	0.333333	4	6	FALSE	CYSLTR1	24.75	4	0	0	0.773256	FALSE	0	CYSLTR1	760	0.399194
145	3.255814	0.033837	0.307143	0	4	6	FALSE	XPA	6.5	4	0	0	0.718023	FALSE	0	XPA	7102	0.289474
155	2.639535	7.02E-06	0.378855	0.833333	4	5	FALSE	FCER2	42.75	4	0	0	0.795058	FALSE	0	FCER2	4	0.521341
159	2.709302	0	0.369099	1	4	5	FALSE	RORA	42.5	4	0	0	0.786337	FALSE	0	RORA	0	0.559211
162	2.848837	8.70E-06	0.35102	0.833333	4	6	FALSE	HLA-B	32.25	4	0	0	0.768895	FALSE	0	HLA-B	4	0.481343
174	3.017442	0.00759	0.331407	0.166667	4	5	FALSE	TNFRSF6B	9.25	4	0	0	0.74782	FALSE	0	TNFRSF6B	1522	0.282258
195	4.244186	0	0.235616	1	4	7	FALSE	LCE1E	6.5	4	0	0	0.594477	FALSE	0	LCE1E	0	0.8125
83	3.372093	4.37E-05	0.296552	0.666667	3	6	FALSE	ALOX12B	9.333333	3	0	0	0.703488	FALSE	0	ALOX12B	6	0.491228
84	2.790698	0.001209	0.358333	0.666667	3	5	FALSE	ZNF148	29.33333	3	0	0	0.776	FA	0	ZNF148	38	0.40740

													163	LSE			0	7
89	3.412791	0.003821	0.293015	0	3	6	FALSE	CCDC80	6.666667	3	0	0	0.6984011	FALSE	0	CCDC80	400	0.333333
95	2.843023	0.003418	0.351738	0	3	5	FALSE	GPC3	20.66667	3	0	0	0.7696622	FALSE	0	GPC3	438	0.357576
101	3.19186	0.01225	0.313297	0	3	5	FALSE	KRIT1	8.333333	3	0	0	0.7260017	FALSE	0	KRIT1	1586	0.333333
103	3.366279	0.011628	0.297064	0.333333	3	6	FALSE	NPRL3	9.333333	3	0	0	0.7042215	FALSE	0	NPRL3	2594	0.428571
106	3.011628	1.49E-05	0.332046	0.666667	3	6	FALSE	PSTPIP2	20	3	0	0	0.7485547	FALSE	0	PSTPIP2	4	0.47619
109	2.77907	0	0.359833	1	3	5	FALSE	CHD7	32.33333	3	0	0	0.7776616	FALSE	0	CHD7	0	0.538889
112	2.825581	0.01626	0.353909	0.333333	3	6	FALSE	PDE4A	28.66667	3	0	0	0.7718002	FALSE	0	PDE4A	2838	0.416667
131	3.581395	7.89E-04	0.279221	0.666667	3	6	FALSE	PDE4B	5.666667	3	0	0	0.6773326	FALSE	0	PDE4B	152	0.435897
138	3.372093	2.40E-04	0.296552	0.333333	3	6	FALSE	GRM4	6	3	0	0	0.7034888	FALSE	0	GRM4	28	0.377778
142	3.465116	0.011918	0.288591	0	3	6	FALSE	RTEL1	4.333333	3	0	0	0.69186	FALSE	0	RTEL1	1634	0.416667
1	3.50581	9.16E-0	0.2852	0.66666	3	6	FAL	HRH1	6	3	0	0	0.6	F	0	HRH1	1	0.5

50	4	5	4	7			SE						86773	ALSE			2	
153	4.162791	0.013418	0.240223	0	3	7	FALSE	RAD9A	2.333333	3	0	0	0.604651	FALSE	0	RAD9A	2610	0.333333
163	3.127907	0	0.319703	1	3	5	FALSE	TBL1XR1	18.33333	3	0	0	0.734012	FALSE	0	TBL1XR1	0	0.572917
168	3.232558	0.002588	0.309353	0	3	6	FALSE	GLB1	6.666667	3	0	0	0.72093	FALSE	0	GLB1	484	0.333333
75	2.918605	0	0.342629	1	2	6	FALSE	KIAA1109	40.5	2	0	0	0.760174	FALSE	0	KIAA1109	0	0.663934
76	3.348837	0.001136	0.298611	0	2	6	FALSE	PRR5L	8.5	2	0	0	0.706395	FALSE	0	PRR5L	166	0.5
79	2.854651	0	0.350306	1	2	5	FALSE	KPNA3	37	2	0	0	0.768169	FALSE	0	KPNA3	0	0.578125
86	3.418605	2.89E-04	0.292517	0	2	6	FALSE	PIEZO1	7	2	0	0	0.697674	FALSE	0	PIEZO1	50	0.5
91	3.255814	0.001102	0.307143	0	2	6	FALSE	IKBKAP	12	2	0	0	0.718023	FALSE	0	IKBKAP	292	0.5
97	3.354651	0.001382	0.298094	0	2	6	FALSE	PPP2R3C	9	2	0	0	0.705669	FALSE	0	PPP2R3C	512	0.5
98	3.47093	3.40E-05	0.288107	0	2	6	FALSE	MFN2	7	2	0	0	0.691134	FALSE	0	MFN2	4	0.666667

102	3.825581	1.55E-04	0.261398	0	2	6	FALSE	CACNA2D2	5	2	0	0	0.646802	FALSE	0	CACNA2D2	20	0.5
125	3.540698	2.88E-04	0.28243	0	2	6	FALSE	PBX2	7.5	2	0	0	0.682413	FALSE	0	PBX2	38	0.5
154	4.395349	0.00231	0.227513	0	2	7	FALSE	RAD50	3	2	0	0	0.575581	FALSE	0	RAD50	196	0.5
180	3.412791	0	0.293015	1	2	6	FALSE	ST14	12	2	0	0	0.698401	FALSE	0	ST14	0	0.6666667
72	4.360465	0	0.229333	0	1	7	FALSE	AP5B1	3	1	0	0	0.579942	FALSE	0	AP5B1	0	0
73	3.656977	0	0.27345	0	1	6	FALSE	SCD	5	1	0	0	0.667878	FALSE	0	SCD	0	0
74	4.116279	0	0.242938	0	1	6	FALSE	STK36	4	1	0	0	0.610465	FALSE	0	STK36	0	0
77	5.156977	0	0.193912	0	1	8	FALSE	EFHC1	3	1	0	0	0.480378	FALSE	0	EFHC1	0	0
78	3.912791	0	0.255572	0	1	7	FALSE	PUS10	6	1	0	0	0.635901	FALSE	0	PUS10	0	0
80	3.226744	0	0.30991	0	1	6	FALSE	FST	23	1	0	0	0.721657	FALSE	0	FST	0	0
81	3.633721	0	0.2752	0	1	7	FALSE	PLA2G7	9	1	0	0	0.67078	FALS	0	PLA2G7	0	0

													5	E				
82	4.273256	0	0.234014	0	1	7	FALSE	ZNF365	6	1	0	0	0.590843	FALSE	0	ZNF365	0	0
85	3.581395	0	0.279221	0	1	6	FALSE	VAX2	13	1	0	0	0.677326	FALSE	0	VAX2	0	0
87	4.087209	0	0.244666	0	1	6	FALSE	TNXB	5	1	0	0	0.614099	FALSE	0	TNXB	0	0
93	2.947674	0	0.33925	0	1	5	FALSE	ANXA6	55	1	0	0	0.756541	FALSE	0	ANXA6	0	0
100	4.186047	0	0.238889	0	1	6	FALSE	RASIP1	3	1	0	0	0.601744	FALSE	0	RASIP1	0	0
108	3.889535	0	0.2571	0	1	7	FALSE	TTC7A	7	1	0	0	0.638808	FALSE	0	TTC7A	0	0
110	4.72093	0	0.211823	0	1	8	FALSE	PDE4C	4	1	0	0	0.534884	FALSE	0	PDE4C	0	0
140	3.534884	0	0.282895	0	1	7	FALSE	CTSE	15	1	0	0	0.68314	FALSE	0	CTSE	0	0
146	4.25	0	0.235294	0	1	7	FALSE	RNF111	4	1	0	0	0.59375	FALSE	0	RNF111	0	0
152	4.087209	0	0.244666	0	1	6	FALSE	COL8A2	5	1	0	0	0.614099	FALSE	0	COL8A2	0	0

Supplement table 3. results from five algorism methods extracted from CytoHubba

Top 50 in network top200 targets string_interactions.tsv ranked by EcCentricity method

Rank	Name	Score
1	EGFR	0.25
1	KRAS	0.25
1	STAT3	0.25
1	CREBBP	0.25
1	MYC	0.25
1	PDGFRB	0.25
1	NR3C1	0.25
1	VDR	0.25
9	NPM1	0.2
9	RELB	0.2
9	BCL2L11	0.2
9	GBA	0.2
9	XBP1	0.2
9	ILK	0.2
9	WAS	0.2
9	FOXC1	0.2
9	FKBP1A	0.2
9	DSG3	0.2
9	ENSG00000196689	0.2
9	TBL1XR1	0.2
9	F3	0.2
9	KPNA3	0.2
9	MMP7	0.2
9	NTRK1	0.2
9	CEBPE	0.2
9	RORA	0.2
9	ITGB2	0.2
9	KIT	0.2
9	IL15RA	0.2
9	KITLG	0.2
9	JAK2	0.2
9	COL5A2	0.2
9	IL4R	0.2
9	LUM	0.2
9	IL13	0.2
9	RXRB	0.2
9	RARA	0.2
9	OVOL1	0.2

9	IL21R	0.2
9	IL21	0.2
9	RXRA	0.2
9	FCER2	0.2
9	REL	0.2
9	NFKBIA	0.2
9	JAK1	0.2
9	FOXP3	0.2
9	ACTL9	0.2
9	IL2	0.2
9	PPIA	0.2
9	RARG	0.2

Top 50 in network top200 targets string_interactions.tsv ranked by EPC method		
Rank	Name	Score
1	IL2	28.258
2	STAT3	27.743
3	IL10	27.507
4	EGFR	27.312
5	IL17A	26.581
6	MYC	25.711
7	FOXP3	25.358
8	IFNG	25.143
9	JAK2	23.656
10	IL7R	23.599
11	IL13	23.586
12	JAK1	23.36
13	JAK3	22.467
14	MAPK14	21.579
15	KRAS	21.024
16	TSLP	20.479
17	PDGFRB	20.275
18	IL4R	19.889
19	LYN	19.877
20	IL21	19.701
21	IL22	19.5
22	KIT	19.258
23	IL6R	19.205
24	ETS1	18.854
25	IL21R	18.791
26	ZAP70	18.509
27	TGFB1	18.402

28	IL12B	18.019
29	KITLG	17.644
30	CREBBP	17.636
31	NFKBIA	17.35
32	FASLG	17.129
33	IL6ST	17.101
34	IL1R1	16.803
35	NR3C1	16.297
36	REL	15.913
37	PTPN22	15.82
38	CD2	15.704
39	MMP1	15.673
40	BCL2L11	14.976
41	RELB	14.953
42	VDR	14.776
43	RARA	13.968
44	ITGAL	13.821
45	ITGB2	13.805
46	ITK	13.671
47	RAF1	13.12
48	MMP13	13.072
49	RB1	12.543
50	NPM1	12.494

303

Top 50 in network top200 targets string interactions.tsv ranked by Degree method		
Rank	Name	Score
1	APP	59
2	KNG1	55
3	C3	45
4	ANXA1	37
5	AGT	35
6	BDKRB1	34
7	C5	31
8	AGTR1	26
9	FN1	25
10	F2	25
11	FGA	25
12	APOA1	24
13	CHRM2	22
13	AHSG	22
15	PTAFR	21
15	HTR1A	21

17	TACR1	21
18	SERPINA1	21
18	HTR2A	20
18	OPRM1	20
21	CHRM1	20
21	OPRK1	20
21	OPRD1	20
24	HRH4	19
24	CHRM4	19
24	APOA2	19
27	CHRM3	19
27	ADRA2C	19
27	ADRA1B	19
30	ADRA1A	19
30	HTR2C	19
32	ADRA2B	19
32	ADRA1D	19
32	ADRA2A	19
32	ADORA3	19
36	CYSLTR1	19
36	APOE	19
36	HRH1	19
36	HTR2B	19
36	TF	19
41	CHRM5	19
41	ADORA1	19
43	PTGDR2	19
43	P4HB	18
43	SERPIND1	18
43	CLU	18
43	APOL1	18
43	A2M	17
49	ALDOA	17
49	ORM2	17

304

Top 50 in network top200 targets string interactions.tsv ranked by MNC method		
Rank	Name	Score
1	APP	59
2	KNG1	55
3	C3	45
3	ANXA1	35
5	AGT	34

6	BDKRB1	34
7	C5	31
8	AGTR1	26
9	F2	24
10	FGA	24
10	APOA1	24
12	FN1	22
13	CHRM2	22
13	AHSG	22
15	TACR1	21
16	SERPINA1	21
16	OPRM1	20
18	OPRK1	20
18	OPRD1	20
18	HRH4	19
21	PTAFR	19
21	HTR1A	19
23	HTR2A	19
23	CHRM4	19
23	APOA2	19
26	CHRM1	19
26	CHRM3	19
26	ADRA2C	19
26	ADRA1B	19
30	ADRA1A	19
31	HTR2C	19
32	ADRA2B	19
32	ADRA1D	19
32	ADRA2A	19
32	ADORA3	19
32	CYSLTR1	19
32	APOE	19
38	HRH1	19
38	HTR2B	19
38	TF	19
41	CHRM5	19
41	ADORA1	19
41	PTGDR2	19
41	SERPIND1	18
45	CLU	18
45	APOL1	18
45	P4HB	17

45	A2M	17
45	ORM2	17
50	APLP2	16

Top 50 in network top200 targets string interactions.tsv ranked by MCC method		
Rank	Name	Score
1	IL2	2.67E+10
2	STAT3	2.67E+10
3	IL10	2.67E+10
4	IFNG	2.67E+10
5	IL13	2.67E+10
6	JAK3	2.66E+10
7	JAK1	2.66E+10
8	JAK2	2.65E+10
9	TSLP	2.65E+10
10	IL22	2.64E+10
11	FOXP3	2.61E+10
12	IL17A	2.52E+10
13	IL6R	1.35E+10
14	IL7R	1.31E+10
15	IL4R	1.30E+10
16	IL21R	1.25E+10
17	EGFR	1.01E+09
18	IL6ST	4.87E+08
19	IL21	1.79E+08
20	PDGFRB	8.29E+07
21	KIT	4.01E+07
22	IL12B	1.96E+07
23	IL1R1	1.54E+07
24	MYC	1586488
25	TGFB1	1231391
26	KITLG	1145700
27	MAPK14	618740
28	ETS1	264632
29	KRAS	220345
30	FASLG	177536
31	CD2	126372
32	NFKBIA	57313
33	ITGAL	45552
34	REL	41232
35	BCL2L11	41073
36	IL18R1	40348

37	RELB	35574
38	ZAP70	24860
39	LYN	20189
40	MMP1	19698
41	CREBBP	16593
42	NR3C1	14000
43	VDR	11379
44	RAF1	10956
45	PTPN22	8396
46	MMP13	7206
47	RARA	6616
48	RXRA	6204
49	RARG	5934
50	RARB	5072

Author Contributions: Conceptualization, writing—review and editing, YS, AWY; review and supervision GBL.

Funding: No funding needed for this project

Acknowledgments: The authors thank Mingdi Li and Hong Li for early versions of the manuscript.

Conflicts of Interest: The authors declare no conflict of interest

Appendix

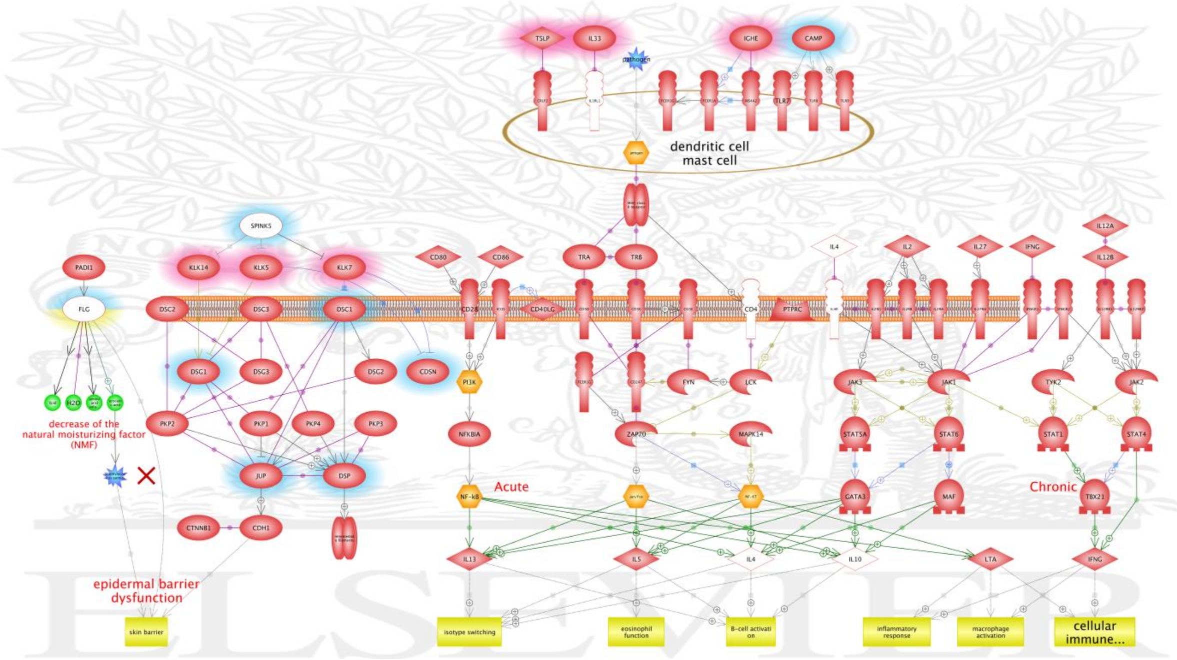

The overview of AD from ELSEVIER Pathway Studio (https://mammalcedfx.pathwaystudio.com/app/search)

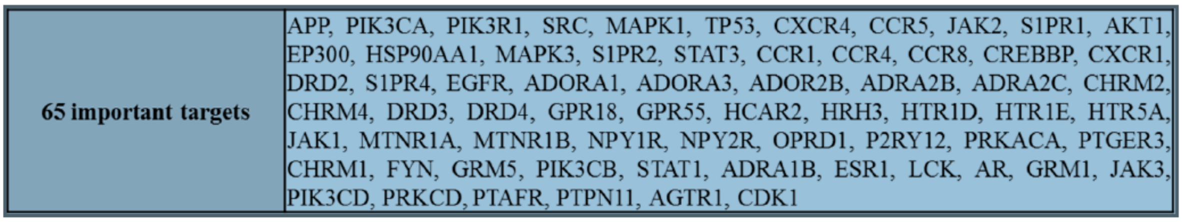

65 important targets	APP, PIK3CA, PIK3R1, SRC, MAPK1, TP53, CXCR4, CCR5, JAK2, S1PR1, AKT1, EP300, HSP90AA1, MAPK3, S1PR2, STAT3, CCR1, CCR4, CCR8, CREBBP, CXCR1, DRD2, S1PR4, EGFR, ADORA1, ADORA3, ADOR2B, ADRA2B, ADRA2C, CHRM2, CHRM4, DRD3, DRD4, GPR18, GPR55, HCAR2, HRH3, HTR1D, HTR1E, HTR5A, JAK1, MTNR1A, MTNR1B, NPY1R, NPY2R, OPRD1, P2RY12, PRKACA, PTGER3, CHRM1, FYN, GRM5, PIK3CB, STAT1, ADRA1B, ESR1, LCK, AR, GRM1, JAK3, PIK3CD, PRKCD, PTAFR, PTPN11, AGTR1, CDK1

The 65 targets associated with pruritus [43]

References

1. Abboud, D.; Hanson, J. Chemokine neutralization as an innovative therapeutic strategy for atopic dermatitis. *Drug Discov. Today* **2017**, *22*, 702-711, doi:10.1016/j.drudis.2016.11.023.

2. Nygaard, U.; Vestergaard, C.; Deleuran, M. Emerging Treatment Options in Atopic Dermatitis: Systemic Therapies. *Dermatology* **2018**, *233*, 344-357, doi:10.1159/000484406.

3. Lee, D.E.; Clark, A.K.; Tran, K.A.; Shi, V.Y. New and emerging targeted systemic therapies: a new era for atopic dermatitis. *The Journal of dermatological treatment* **2018**, *29*, 364-374, doi:10.1080/09546634.2017.1373736.

4. Rerknimitr, P.; Otsuka, A.; Nakashima, C.; Kabashima, K. The etiopathogenesis of atopic dermatitis: barrier disruption, immunological derangement, and pruritus. *Inflammation and regeneration* **2017**, *37*, 14, doi:10.1186/s41232-017-0044-7.

5. Carroll, C.L.; Balkrishnan, R.; Feldman, S.R.; Fleischer Jr, A.B.; Manuel, J.C. The burden of atopic dermatitis: impact on the patient, family, and society. *Pediatr. Dermatol.* **2005**, *22*, 192-199.

6. Wang, D.; Beck, L.A. Immunologic Targets in Atopic Dermatitis and Emerging Therapies: An Update. *Am. J. Clin. Dermatol.* **2016**, *17*, 425-443, doi:10.1007/s40257-016-0205-5.

7. Kou, Y.; Zhang, S.; Chen, X.; Hu, S. Gene expression profile analysis of colorectal cancer to investigate potential mechanisms using bioinformatics. *Onco Targets Ther.* **2015**, *8*, 745-752, doi:10.2147/ott.S78974.

8. Bao, L.; Zhang, H.; Chan, L.S. The involvement of the JAK-STAT signaling pathway in chronic inflammatory skin disease atopic dermatitis. *Jakstat* **2013**, *2*, e24137, doi:10.4161/jkst.24137.

9. Sarra, M.; Franze, E.; Pallone, F.; Monteleone, G. Targeting interleukin-21 in inflammatory diseases. *Expert Opin. Ther. Targets* **2011**, *15*, 695-702, doi:10.1517/14728222.2011.561319.

10. Schmitt, J.; Schwarz, K.; Baurecht, H.; Hotze, M.; Folster-Holst, R.; Rodriguez, E.; Lee, Y.A.E.; Franke, A.; Degenhardt, F.; Lieb, W., et al. Atopic dermatitis is associated with an increased risk for rheumatoid arthritis and inflammatory bowel disease, and a decreased risk for type 1 diabetes. *J. Allergy Clin. Immunol.* **2016**, *137*, 130-136, doi:10.1016/j.jaci.2015.06.029.

11. Kim, H.S.; Jang, S.W.; Lee, W.; Kim, K.; Sohn, H.; Hwang, S.S.; Lee, G.R. PTEN drives Th17 cell differentiation by preventing IL-2 production. *J. Exp. Med.* **2017**, *214*, 3381-3398, doi:10.1084/jem.20170523.

12. Chandra, V.; Huang, P.; Hamuro, Y.; Raghuram, S.; Wang, Y.; Burris, T.P.; Rastinejad, F. Structure of the intact PPAR-gamma-RXR- nuclear receptor complex on DNA. *Nature* **2008**, *456*, 350-356, doi:10.1038/nature07413.

13. Hanifin, J.M.; Stevens, V.; Sheth, P.; Breneman, D. Novel treatment of chronic severe hand dermatitis with bexarotene gel. *Br. J. Dermatol.* **2004**, *150*, 545-553, doi:10.1046/j.1365-2133.2003.05729.x.

14. Melnik, B.C. The potential role of impaired Notch signalling in atopic dermatitis. *Acta Derm. Venereol.* **2015**, *95*, 5-11, doi:10.2340/00015555-1898.

15. Bao, L.; Alexander, J.B.; Zhang, H.; Shen, K.; Chan, L.S. Interleukin-4 Downregulation of Involucrin Expression in Human Epidermal Keratinocytes Involves Stat6 Sequestration of the Coactivator CREB-Binding Protein. *J. Interferon Cytokine Res.* **2016**, *36*, 374-381, doi:10.1089/jir.2015.0056.

16. Zhang, Z.K.; Yang, Y.; Bai, S.R.; Zhang, G.Z.; Liu, T.H.; Zhou, Z.; Wang, C.M.; Tang, L.J.; Wang, J.; He, S.X. Screening for key genes associated with atopic dermatitis with DNA microarrays. *Mol Med Rep* **2014**, *9*, 1049-1055, doi:10.3892/mmr.2014.1908.

17. Heine, G.; Hoefer, N.; Franke, A.; Nothling, U.; Schumann, R.R.; Hamann, L.; Worm, M. Association of vitamin D receptor gene polymorphisms with severe atopic dermatitis in adults. *Br. J. Dermatol.* **2013**, *168*, 855-858, doi:10.1111/bjd.12077.

18. Kanbe, T.; Soma, Y.; Kawa, Y.; Kashima, M.; Mizoguchi, M. Serum levels of soluble stem cell factor and soluble KIT are elevated in patients with atopic dermatitis and correlate with the disease severity. *Br. J. Dermatol.* **2001**, *144*, 1148-1153.

19. Sionov, R.V.; Vlahopoulos, S.A.; Granot, Z. Regulation of Bim in Health and Disease. *Oncotarget* **2015**, *6*, 23058-23134, doi:10.18632/oncotarget.5492.

20. Hirota, T.; Takahashi, A.; Kubo, M.; Tsunoda, T.; Tomita, K.; Sakashita, M.; Yamada, T.; Fujieda, S.; Tanaka, S.; Doi, S., et al. Genome-wide association study identifies eight new susceptibility loci for atopic dermatitis in the Japanese population. *Nat. Genet.* **2012**, *44*, 1222-1226, doi:10.1038/ng.2438.

21. Tanaka, A.; Muto, S.; Jung, K.; Itai, A.; Matsuda, H. Topical application with a new NF-kappaB inhibitor improves atopic dermatitis in NC/NgaTnd mice. *J. Invest. Dermatol.* **2007**, *127*, 855-863, doi:10.1038/sj.jid.5700603.

22. Chen, R.F.; Chang, C.H.; Wang, C.T.; Yang, M.Y.; Wang, C.J.; Kuo, Y.R. Modulation of vascular endothelial growth factor and mitogen-activated protein kinase-related pathway involved in extracorporeal shockwave therapy accelerate diabetic wound healing. *Wound Repair Regen.* **2019**, *27*, 69-79, doi:10.1111/wrr.12686.

23. Samochocki, Z.; Bogaczewicz, J.; Sysa-Jedrzejowska, A.; McCauliffe, D.P.; Kontny, E.; Wozniacka, A. Expression of vascular endothelial growth factor and other cytokines in atopic dermatitis, and correlation with clinical features. *Int. J. Dermatol.* **2016**, *55*, e141-146, doi:10.1111/ijd.13132.

24. Moradkhani, S.; Jafarzadeh, A.; Bazargan-Harandi, N.; Baneshi, M.R.; Mohammadi, M.M. Association of reduced count of interleukin-13-producing cells in breast milk with atopic dermatitis in infancy. *Indian J. Med. Res.* **2018**, *148*, 317-322, doi:10.4103/ijmr.IJMR_1682_16.

25. Hamann, C.R.; Thyssen, J.P. Monoclonal antibodies against interleukin 13 and interleukin 31RA in development for atopic dermatitis. *J. Am. Acad. Dermatol.* **2018**, *78*, S37-s42, doi:10.1016/j.jaad.2017.12.018.

26. Cotter, D.G.; Schairer, D.; Eichenfield, L. Emerging therapies for atopic dermatitis: JAK inhibitors. *J. Am. Acad. Dermatol.* **2018**, *78*, S53-s62, doi:10.1016/j.jaad.2017.12.019.

27. Lyu, Y.; Zhu, L.; Qi, R.; Xu, J.; Di, Z.; Chen, H.; Gao, X. Serum levels of suppressor of cytokine signaling 3 and signal transducer and activator of transcription 3 in childhood atopic dermatitis. *Chin. Med. J. (Engl.)* **2014**, *127*, 2389-2391.

28. Mollanazar, N.K.; Smith, P.K.; Yosipovitch, G. Mediators of Chronic Pruritus in Atopic Dermatitis: Getting the Itch Out? *Clin. Rev. Allergy Immunol.* **2016**, *51*, 263-292, doi:10.1007/s12016-015-8488-5.

29. Christensen, U.; Haagerup, A.; Binderup, H.G.; Vestbo, J.; Kruse, T.A.; Borglum, A.D. Family based association analysis of the IL2 and IL15 genes in allergic disorders. *Eur. J. Hum. Genet.* **2006**, *14*, 227-235, doi:10.1038/sj.ejhg.5201541.

30. Kraft, M.; Worm, M. Dupilumab in the treatment of moderate-to-severe atopic dermatitis. *Expert Rev. Clin. Immunol.* **2017**, *13*, 301-310, doi:10.1080/1744666x.2017.1292134.

31. Costanzo, A.; Chimenti, M.S.; Botti, E.; Caruso, R.; Sarra, M.; Monteleone, G. IL-21 in the pathogenesis and treatment of skin diseases. *J. Dermatol. Sci.* **2010**, *60*, 61-66, doi:10.1016/j.jdermsci.2010.08.016.

32. Dieckhoff, K.; Graf, P.; Beinhauer, B.; Schwaerzler, C.; Carballido, J.M.; Neumann, C.; Zachmann, K.; Jung, T. Deficient translocation of c-Rel is associated with impaired Th1 cytokine production in T cells from atopic dermatitis patients. *Exp. Dermatol.* **2005**, *14*, 17-25, doi:10.1111/j.0906-6705.2005.00241.x.

33. Barton, D.; HogenEsch, H.; Weih, F. Mice lacking the transcription factor RelB develop T cell-dependent skin lesions similar to human atopic dermatitis. *Eur. J. Immunol.* **2000**, *30*, 2323-2332, doi:10.1002/1521-4141(2000)30:8<2323::Aid-immu2323>3.0.Co;2-h.

34. Yamada, K.; Hamashima, T.; Ishii, Y.; Yamamoto, S.; Okuno, N.; Yoshida, N.; Yamada, M.; Huang, T.T.; Shioda, N.; Tomihara, K., et al. Different PDGF Receptor Dimers Drive Distinct Migration Modes of the Mouse Skin Fibroblast. *Cell. Physiol. Biochem.* **2018**, *51*, 1461-1479, doi:10.1159/000495594.

35. El Samahy, M.H.; Attia, E.A.; Saad, A.A.; Mahmoud, E.Y. Circulating CD4(+) CD25(high) FoxP3(+) T-regulatory cells in patients with atopic dermatitis after narrowband-ultraviolet B phototherapy. *Int. J. Dermatol.* **2015**, *54*, e424-429, doi:10.1111/ijd.12801.

36. Lee, G.R.; Maarouf, M.; Hendricks, A.K.; Lee, D.E.; Shi, V.Y. Current and emerging therapies for hand eczema. *Dermatol. Ther.* **2019**, 10.1111/dth.12840, e12840, doi:10.1111/dth.12840.

37. Choi, S.Y.; Lee, Y.J.; Kim, J.M.; Kang, H.J.; Cho, S.H.; Chang, S.E. Epidermal Growth Factor Relieves Inflammatory Signals in Staphylococcus aureus-Treated Human Epidermal Keratinocytes and Atopic Dermatitis-Like Skin Lesions in Nc/Nga Mice. *BioMed research international* **2018**, *2018*, 9439182, doi:10.1155/2018/9439182.

38. Shi, Y.; Xu, X.; Zhang, Q.; Fu, G.; Mo, Z.; Wang, G.S.; Kishi, S.; Yang, X.L. tRNA synthetase counteracts c-Myc to develop functional vasculature. *eLife* **2014**, *3*, e02349, doi:10.7554/eLife.02349.

39. Kim, J.Y.; Cho, Y.E.; Park, J.H. The Nucleolar Protein GLTSCR2 Is an Upstream Negative Regulator of the Oncogenic Nucleophosmin-MYC Axis. *Am. J. Pathol.* **2015**, *185*, 2061-2068, doi:10.1016/j.ajpath.2015.03.016.

40. Deckers, J.; Bougarne, N.; Mylka, V.; Desmet, S.; Luypaert, A.; Devos, M.; Tanghe, G.; Van Moorleghem, J.; Vanheerswynghels, M.; De Cauwer, L., et al. Co-Activation of Glucocorticoid Receptor and Peroxisome Proliferator-Activated Receptor-gamma in Murine Skin Prevents Worsening of Atopic March. *J. Invest. Dermatol.* **2018**, *138*, 1360-1370, doi:10.1016/j.jid.2017.12.023.

41. Zappia, C.D.; Granja-Galeano, G.; Fernandez, N.; Shayo, C.; Davio, C.; Fitzsimons, C.P.; Monczor, F. Effects of histamine H1 receptor signaling on glucocorticoid receptor activity. Role of canonical and non-canonical pathways. *Sci. Rep.* **2015**, *5*, 17476, doi:10.1038/srep17476.

42. Zhong, J.; Liu, Z.; Zhou, X.; Xu, J. Synergic Anti-Pruritus Mechanisms of Action for the Radix Sophorae Flavescentis and Fructus Cnidii Herbal Pair. *Molecules* **2017**, *22*, doi:10.3390/molecules22091465.